

# Structural Studies of Hyaluronan Hydrogels

Frida J. Wende

*Faculty of Natural Resources and Agricultural Sciences*

*Department of Molecular Sciences*

*Uppsala*

Doctoral thesis

Swedish University of Agricultural Sciences

Uppsala 2019

Acta Universitatis agriculturae Sueciae

2019:30

Cover: Schematic representation of the structure of a hyaluronan hydrogel with mono- and double-linked 1,4-butanediol diglycidyl ether

ISSN 1652-6880

ISBN (print version) 978-91-7760-378-8

ISBN (electronic version) 978-91-7760-379-5

© 2019 Frida J. Wende, Uppsala

Print: SLU Service/Repro, Uppsala 2019

# Structural Studies of Hyaluronan Hydrogels

## Abstract

Hydrogels consist of cross-linked polymer networks with the ability to absorb large amounts of water. In this thesis, the structures of hydrogels consisting of hyaluronic acid (HA) cross-linked by 1,4-butanediol diglycidyl ether (BDDE) have been investigated. Hyaluronic acid is a naturally occurring polysaccharide that is abundant in the extracellular matrix of all vertebrates. Due to high viscoelasticity and biocompatibility, hyaluronic acid based hydrogels have many biomedical applications.

Nuclear magnetic resonance (NMR) spectroscopy and mass spectrometry (MS), which are among the most important analytical techniques for analysis of organic compounds and biomacromolecules, were used for analysis of structural properties of HA-BDDE hydrogels.

NMR- and MS-based methods were developed to determine the positions of substitution of the cross-linker on HA in fragments obtained from enzymatic degradation of HA-BDDE hydrogels. One-dimensional proton and carbon NMR methods were then further developed for quantitative analysis of substitution positions, degree of modification and degree of cross-linking. No chromatographic separation step was needed.

Desulphated chondroitin has a primary structure that only differs from that of HA by the configuration at C4 of the aminoglycan. The reactivity of desulphated chondroitin towards BDDE as well as alkali-induced changes in chemical shifts were determined and compared to that of hyaluronic acid. Using NMR spectroscopy of hydroxyl protons, hydrogen bonding in the two polymers were compared.

Water is the most abundant component of the studied hydrogels. Using NMR spectroscopy, the relaxation and diffusion behaviour of water protons in native HA solutions and cross-linked HA hydrogels with different physicochemical properties were studied. The transverse relaxation, which is dominated by chemical exchange, could be correlated to polysaccharide mobility.

*Keywords:* Hyaluronan, NMR spectroscopy, mass spectrometry, polysaccharide, glycosaminoglycan, cross-linking, hydrogel

*Author's address:* Frida Wende, SLU, Department of Molecular Sciences,

P.O. Box 7015, 750 07 Uppsala, Sweden

*E-mail:* frida.wende@slu.se

# Dedication

To William, Douglas & Olivia

*Nothing can dim the light that shines from within.*

-Maya Angelou

# Contents

<b>List of publications</b>	<b>7</b>
<b>Abbreviations</b>	<b>9</b>
<b>1 Introduction</b>	<b>11</b>
<b>2 Hyaluronic acid</b>	<b>13</b>
2.1 Structure of HA	14
2.2 Chemical modification of HA structure	16
2.2.1 Cross-linking	16
2.2.2 Modified HA for drug delivery	17
2.3 Enzymatic and chemical degradation of HA	18
2.3.1 Hydrolases (EC 3.2.1.-)	18
2.3.2 Lyases (EC 4.2.2.-)	19
2.3.3 Non-enzymatic degradation	20
2.4 Analysis of physical and chemical properties of HA-BDDE hydrogels	20
<b>3 Chondroitin</b>	<b>25</b>
<b>4 Methods</b>	<b>26</b>
4.1 NMR Spectroscopy	26
4.1.1 Principle	26
4.1.2 Relaxation	29
4.1.3 NMR for studies of carbohydrates	29
4.1.4 Exchangeable protons	34
4.1.5 Non-uniform sampling	35
4.1.6 Determination of relaxation parameters	37
4.1.7 Diffusion NMR spectroscopy	39
4.2 Mass Spectrometry	41
4.2.1 Ionisation	42
4.2.2 Mass analysers	43
4.2.3 Fragmentation	45
<b>5 Aims</b>	<b>47</b>

<b>6</b>	<b>Results and discussion</b>	<b>48</b>
6.1	BDPE substitution positions in HA hydrogels – elucidation and method development (Papers I-II)	48
6.1.1	Elucidation of substitution positions by NMR	48
6.1.2	Elucidation of substitution positions by MS	51
6.1.3	Configuration of BDPE	54
6.1.4	Development of 1D <sup>1</sup> H NMR method for quantification of substitution positions in HA hydrogels	54
6.2	1D <sup>13</sup> C NMR method for determination of degree of cross-linking (Paper II)	56
6.3	Comparison of reactivity of HA and CN toward BDDE and alkali induced changes (Paper III)	59
6.3.1	Substitution positions of BDPE on CN	59
6.3.2	Alkali induced changes in <sup>1</sup> H and <sup>13</sup> C chemical shifts	62
6.3.3	NMR of exchangeable protons	63
6.4	Relaxation and diffusion of water protons in HA solutions and hydrogels – comparison with physicochemical parameters (Paper IV)	64
6.4.1	Longitudinal relaxation ( <i>T</i> <sub>1</sub> ) and diffusion coefficient ( <i>D</i> ) of water protons	65
6.4.2	Transverse relaxation ( <i>T</i> <sub>2</sub> ) of water protons	66
<b>7</b>	<b>Conclusion and future perspectives</b>	<b>68</b>
	<b>References</b>	<b>70</b>
	<b>Popular science summary</b>	<b>79</b>
	<b>Populärvetenskaplig sammanfattning</b>	<b>81</b>
	<b>Acknowledgements</b>	<b>83</b>

## List of publications

This thesis is based on the work contained in the following papers, referred to by Roman numerals in the text:

- I Frida J. Wende, Suresh Gohil, Hotan Mojarradi, Thibaud Gerfaud, Lars I. Nord, Anders Karlsson, Jean-Guy Boiteau, Anne Helander Kenne, Corine Sandström. (2016). Determination of substitution positions in hyaluronic acid hydrogels using NMR and MS based methods. *Carbohydrate Polymers*, 136, 1348-1357.
- II Frida J. Wende, Suresh Gohil, Lars I. Nord, Anne Helander Kenne, Corine Sandström. (2017). 1D NMR methods for determination of degree of cross-linking and BDDE substitution positions in HA hydrogels. *Carbohydrate Polymers*, 157, 1525-1530.
- III Frida J. Wende, Suresh Gohil, Lars I. Nord, Anders Karlsson, Anne Helander Kenne, Corine Sandström. (2019). Insights on the reactivity of chondroitin and hyaluronan toward 1,4-butanediol diglycidyl ether. *International Journal of Biological Macromolecules*, 131, 812-820.
- IV Frida J. Wende, Gustav Nestor, Åke Öhrlund, Corine Sandström. Relaxation and diffusion of water protons in BDDE cross-linked hyaluronic acid hydrogels investigated by NMR spectroscopy – comparison with physicochemical properties (Manuscript)

Papers I-III are reproduced with the permission of the publishers.

The contribution of Frida Wende to the papers included in this thesis was as follows:

- I Project planning and discussion together with co-authors. NMR analysis and interpretation of NMR and MS data. Writing the manuscript with co-authors.
- II Project planning and discussion together with co-authors. Sample preparation, NMR analysis and interpretation of data. Writing the manuscript with co-authors.
- III Project planning and discussion together with co-authors. Sample preparation, NMR and MS analysis and interpretation of data. Writing the manuscript with co-authors.
- IV Project planning and discussion together with co-authors. Sample preparation, NMR analysis, processing and interpretation of data. Writing the manuscript with co-authors.

## Abbreviations

BDDE	1,4-ButaneDiol Diglycidyl Ether
BDPE	1,4-ButaneDiol di-(Propan-2,3-diolyl)Ether
chABC	chondroitinase ABC
CID	Collision Induced Dissociation
CI	Chemical Ionisation
CN	desulphated chondroitin
$\Delta\text{CN}_x$	CN oligosaccharide containing x monosaccharides with non-reducing end $\Delta\text{GlcA}$
$\Delta\text{CN}_x\text{-B}$	CN oligosaccharide containing x monosaccharides linked to BDPE with non-reducing end $\Delta\text{GlcA}$
COSY	CORrelation SpectroscopY
CPD	Composite Pulse Decoupling
CPMG	Carr-Purcell-Meiboom-Gill
CrD	Degree of Cross-linking
CrR	effective Cross-linker Ratio
CS	Chondroitin Sulphate
DC	Degree of Cross-linking
DMSO	DiMethyl SulfOxide
DS	Degree of Substitution
EI	Electron Ionisation
EIC	Extracted Ion Chromatogram
ESI	ElectroSpray Ionisation
ETD	Electron Transfer Dissociation
FID	Free Induction Decay
FT	Fourier Transform
GAG	GlycosAminoGlycan
GalNAc	<i>N</i> -acetyl-D-galactosamine

GlcNAc	<i>N</i> -acetyl-D-glucosamine
GlcA	D-Glucuronic acid
$\Delta$ GlcA	D-Glucuronic acid with C4-C5 unsaturation
GC	Gas Chromatography
HA	Hyaluronic Acid/Hyaluronan/Hyaluronate
HA <sub>x</sub>	HA oligosaccharide containing x monosaccharides
$\Delta$ HA <sub>x</sub>	HA oligosaccharide containing x monosaccharides with non-reducing end $\Delta$ GlcA
$\Delta$ HA <sub>x</sub> -B	HA oligosaccharide containing x monosaccharides linked to BDPE with non-reducing end $\Delta$ GlcA
HMBC	Heteronuclear Multiple Bond Correlation
HSQC	Heteronuclear Single Quantum Coherence
IT	Ion Trap
LC	Liquid Chromatography
MALDI	Matrix Assisted Laser Desorption Ionisation
MD	Molecular Dynamics
MoD	Degree of Modification
MS	Mass Spectrometry
MW	Molecular Weight
NMR	Nuclear Magnetic Resonance
NOE	Nuclear Overhauser Effect
NOESY	Nuclear Overhauser Effect Spectroscopy
NUS	Non-Uniform Sampling
PGSE	Pulsed Gradient Spin Echo
RF	Radio Frequency
RNS	Reactive Nitrogen Species
ROS	Reactive Oxygen Species
SEC	Size Exclusion Chromatography
SEM	Scanning Electron Microscopy
TIC	Total Ion Chromatogram
TOCSY	TOTAL Correlation Spectroscopy
TOF	Time Of Flight

# 1 Introduction

Hydrogels are cross-linked polymer networks in three dimensions that are able to absorb large amounts of water. The polymers can be either chemically or physically cross-linked *e.g.* by entanglements (Hoffman, 2012). Cross-linked hyaluronic acid (HA) is due to its inherent biocompatibility one of the most common hydrogels used for biomedical applications (Tiwari & Bahadur, 2019). HA derivatives are available for soft tissue augmentation, tissue engineering, joint lubrication (to reduce friction in osteoarthritis), treatment of a range of ocular disease and as a carrier for drug delivery (Kim *et al.*, 2017). The *in vivo* duration of HA can be improved by chemical modification (*e.g.* cross-linking) and one of the most common hydrogels is HA cross-linked with 1,4-butanediol diglycidyl ether (BDDE). There are several manufacturers of HA-BDDE hydrogels offering a wide range of products, which present a great variation in gel properties.

Inherent sources of differences in properties are the concentrations and proportion of HA and BDDE as well as the molecular weight of the HA starting material. The amount of modification and cross-linking will depend on the efficiency of the manufacturing process. These parameters will in turn affect the physical properties of the hydrogels. Other factors such as position of substitution of the cross-linker on the polysaccharide and cross-link distribution might also be important. To be able to design hydrogels with desired physicochemical properties, their relationship with chemical parameters and the manufacturing process must be understood. To achieve this robust analytical methods are required.

Thus, the main focus of this thesis has been to study the structure and properties of cross-linked HA-BDDE hydrogels and to create methods for analysis and comparison of these properties to distinguish between different hydrogels. The substitution positions of BDDE on HA was determined (Paper I) and simple one-dimensional proton and carbon nuclear magnetic resonance (NMR) methods for analysis of the substitution position with simultaneous

analysis of degree of modification and degree of cross-linking were developed (Paper II). In an attempt to explain the preference of position of substitution of BDDE on HA, the reactivity of desulphated chondroitin towards BDDE and alkali was investigated in Paper III and compared to that of HA. Hydrogen bonding in the two polymers were also compared. Finally, since the major constituent of HA-BDDE hydrogels is water, the self-diffusion and relaxation behaviour of water protons in hydrogels and solutions of HA were studied by NMR spectroscopy (Paper IV).

## 2 Hyaluronic acid

Hyaluronic acid (HA) is a naturally occurring polysaccharide (carbohydrate polymer). Meyer and Palmer, who first isolated HA from the vitreous humour of bovine eye, named it “hyaluronic acid” from hyaloid (Greek *ύαλοειδής* meaning glassy or transparent) and uronic acid (Meyer & Palmer, 1934). Balazs *et al.* suggested that the name “hyaluronic acid” should be used for the molecule in acid form while “hyaluronate” should be used for the polyanionic form. However, the acid is often partially dissociated and thus the term “hyaluronan” was suggested as a general nomenclature for the polysaccharide independently of the degree of dissociation (Balazs *et al.*, 1986). In this thesis, I will use the abbreviation HA for convenience.

In humans, HA is an important component of the extracellular matrix. It is most abundant in the umbilical cord, vitreous body of the eye and in the synovial fluid. The skin and joints also carry high concentrations of HA. All tissues and tissue fluids contain HA but of varying sizes and different concentrations. The lowest concentration has been found in human serum (Laurent, 1987). An adult weighing 70 kg contains about 15 g of HA in total of which approximately half (7-8 g) is found in skin tissue (Fraser & Laurent, 1989; Stern & Maibach, 2008).

For biomedical use, HA can be derived either from animal sources (most commonly rooster combs or bovine eyes) or from bacterial fermentation (Sze *et al.*, 2016). Rooster combs are used since they have the highest concentration of HA (7.5 mg/ml) compared to all other animal tissues (Laurent & Fraser, 1992). The extraction and purification from rooster combs is time consuming and contaminations by proteoglycans and HA degrading enzymes are hard to avoid. Production of HA from bacterial fermentation has thus grown as an important source of the polysaccharide. Bacteria used for production of HA are gram-positive *Streptococcus zooepidemicus* (among other members of streptococci groups A and C) (Zakeri *et al.*, 2017) and gram-negative *Pasteurella multocida* (DeAngelis *et al.*, 1998). The truncated form of the hyaluronan synthase from *P. multocida* has been utilised for cell free HA production. It has proved to produce

HA of very low polydispersity (DeAngelis, 2008), and through directed evolution also of very high molecular weight (Mandawe *et al.*, 2018).

The molecular weight of HA can reach up to 12 MDa when isolated from naked mole rats. Skin from humans, rabbits and rats contains HA with molecular weight in the range 4-6 MDa (Cowman *et al.*, 2015). HA produced by fermentation is available in < 3 MDa, but production of higher molecular weight polymers has been reported (Rangaswamy & Jain, 2008; Im *et al.*, 2009; Mandawe *et al.*, 2018).

Depending on the molecular weight, HA has different biological effects and therefore both the polymer synthesis and the extent of *in vivo* degradation are of great importance. High molecular weight HA exerts anti-inflammatory, anti-angiogenic, and immunosuppressive effects. It is involved in biological processes such as tissue regeneration, wound repair, ovulation and embryogenesis. High molecular weight HA is highly viscous and viscoelastic, and protects cartilage by acting as a lubricant in the synovial fluid (Stern *et al.*, 2006). Low molecular weight HA, on the other hand, has opposite effects, *i.e.* pro-inflammatory, pro-angiogenic and immunostimulatory (Stern *et al.*, 2006). Despite many studies devoted to understanding of the diverse biological roles of HA, everything is not fully understood and more research is needed (Dicker *et al.*, 2014; Fallacara *et al.*, 2018).

## 2.1 Structure of HA

HA belongs to a family of unbranched polysaccharides called glycosaminoglycans (GAGs). The repeating unit of a GAG consists of an uronic acid and an amino sugar (either *N*-acetylglucosamine, GlcNAc or *N*-acetylgalactosamine, GalNAc). For HA, the repeating unit is  $\beta$ -D-GlcA-(1 $\rightarrow$ 3)- $\beta$ -D-GlcNAc-(1 $\rightarrow$ 4) (Figure 1). HA is the only GAG that does not occur with any degree of sulphation meaning that the primary structure is always preserved and the only variation of natural HA is the molecular weight and the polydispersity. Other members of the GAG family are chondroitin sulphate, dermatan sulphate, heparin, heparin sulphate and keratin sulphate.

The uronic acids of HA have a  $pK_a$  around 3 (Tømmeraas & Wahlund, 2009) resulting in a polyanion at neutral pH.

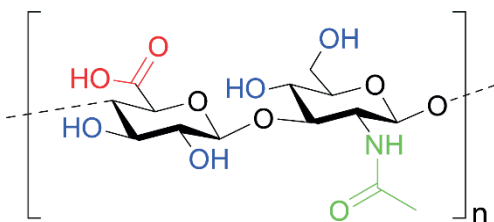


Figure 1. Repeating unit of hyaluronic acid  $\rightarrow(4)\text{-}\beta\text{-D-GlcA-(1}\rightarrow\text{3)-}\beta\text{-D-GlcNAc-(1}\rightarrow$ . The six functional groups available for chemical modification are: i) hydroxyls (blue), ii) carboxylic acid (red), and iii) acetamido group (green).

The higher order structures of HA are much more complex than the primary structure. Many studies have been devoted to decipher the three-dimensional conformation in solution and in solid state, with sometimes contradictory results. The structure of HA in the solid state has been investigated by both X-ray diffraction and NMR spectroscopy (Hargittai & Hargittai, 2008). The structure of HA in solution has been investigated by NMR spectroscopy and predicted by molecular dynamics (MD) simulations (Pomin, 2014). Other experimental approaches such as rheological, microscopic and light scattering have been used to gain more insight on the HA structure (Cowman & Matsuoka, 2005). Several different types of helical structures have been identified in the solid state (Haxaire *et al.*, 2000) and it can be concluded that the structure is influenced by temperature, type of counter ion, ionic strength, humidity and pH (Sheehan & Atkins, 1983). All the described structures are stabilised by hydrogen bonds. Left-handed helical structures have been suggested from NMR studies in combination with MD simulations of aqueous HA oligosaccharides (Holmbeck *et al.*, 1994; Almond *et al.*, 2006; Gargiulo *et al.*, 2010). A comparison between HA in solution and in solid state by  $^{13}\text{C}$  NMR revealed significant differences indicating loss of inter- and/or intramolecular hydrogen bonds and a change in chain conformation (Feder-Davis *et al.*, 1991). It is likely that the *in vivo* conformation of HA is affected by the local environment (*e.g.* ionic strength, interactions with ions and macromolecules, excluded volume) and that the different conformations contribute to the diverse biological functions of HA together with its size (Gargiulo *et al.*, 2010).

The viscoelasticity of HA solutions suggest an inherent chain stiffness along with inter-chain interactions. Intra-molecular hydrogen bonds have been detected over both glycosidic linkages. Up to five intramolecular hydrogen bonds (A-E in Figure 2) have been suggested from NMR and MD simulation studies (Scott *et al.*, 1984; Heatley & Scott, 1988; Almond, 2005; Nestor *et al.*, 2010) as well as from X-ray diffraction studies (Guss *et al.*, 1975; Mitra *et al.*, 1983). In aqueous solution, hydrogen bond E is suggested to be replaced by a

water bridge (Heatley & Scott, 1988). The hydrogen bonds A and B are more frequently observed suggesting that the other three are weaker if present. All hydrogen bonds in aqueous solutions are however short lived allowing for segmental motion of the HA chain. Although HA as a whole is extremely hydrophilic there is a hydrophobic surface formed by the axial hydrogens while the equatorial groups form a hydrophilic surface (Scott, 1989).

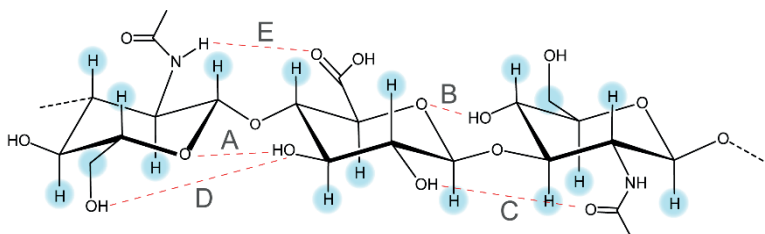


Figure 2. Schematic representation of HA trisaccharide (GlcNAc-GlcA-GlcNAc) showing the five hydrogen bonds (A-E) discussed in the literature.

## 2.2 Chemical modification of HA structure

Chemical modification of HA is a common approach to produce biomaterials with desired biological effects and physicochemical properties (*e.g.* prolonged *in vivo* duration, altered viscoelasticity or therapeutic actions) (Schanté *et al.*, 2011; Tiwari & Bahadur, 2019). The repeating unit of HA has several possible targets for chemical modification: four hydroxyl groups, one carboxylic acid and one acetamido group (Figure 1).

### 2.2.1 Cross-linking

To increase *in vivo* duration and viscosity, HA is often cross-linked by low molecular weight compounds with two functional groups. These bifunctional molecules can react with HA on both sides of the cross-linker to create linkages between HA chains and thereby building up a network that is more resistant to degradation.

There have been numerous successful attempts to produce cross-linked HA targeting all three types of handles (hydroxyls, carboxylic acid and acetamide group) on the HA repeating unit (Figure 1) (Khunmanee *et al.*, 2017). Using the hydroxyls as target, formation of ether bonds can be achieved by reaction with diepoxides (Tomihata & Ikada, 1997b; Ågerup, 1998; Segura *et al.*, 2005) or divinyl sulfone (Balazs & Leshchiner, 1986). Esterification (Larrañeta *et al.*, 2018) and hemiacetal formation by reaction with glutaraldehyde (Tomihata & Ikada, 1997a) are other possible reactions targeting the hydroxyl groups.

One of the most common cross-linkers for HA hydrogels is 1,4-butanediol diglycidyl ether (BDDE, Figure 3) (Khunmanee *et al.*, 2017). Under alkaline conditions, the hydroxyl groups of HA are deprotonated and the resulting alkoxide anions can act as nucleophiles and attack the epoxides of BDDE (Figure 3). The ring opening produces derivatives of 1,4-butanediol di-(propan-2,3-diolyl)ether (BDPE). When one BDDE reacts with two HA chains, a “double-linked” BDPE is formed. However, the BDDE epoxides can also react with water resulting in “mono-linked” BDPE (Figure 3) or free BDPE. The covalent ether bond that is formed between HA and BDPE is stable towards degradation (De Boulle *et al.*, 2013).

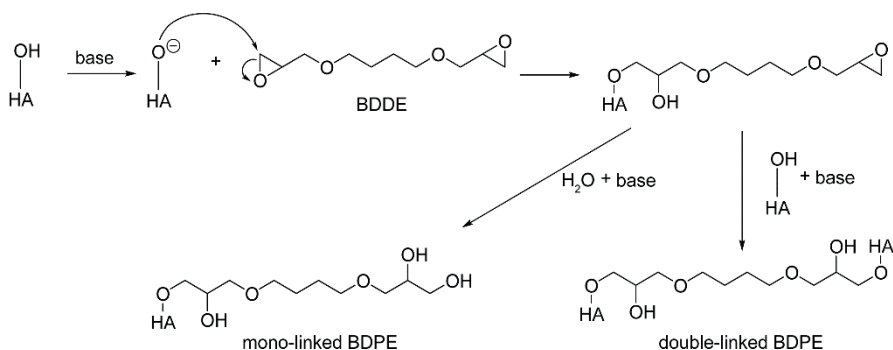


Figure 3. Cross-linking of HA with BDDE under alkaline conditions will result in some true cross-links (double-linked BDPE) and some pendant cross-linkers (mono-linked BDPE).

The carboxylic acid is a good target for amidation with diamines (Barbucci *et al.*, 2000; Barbucci *et al.*, 2003) or dihydrazides (Luo *et al.*, 2000a), and for esterification (Huin-Amargier *et al.*, 2006), oxidation (Jia *et al.*, 2004), and Ugi condensation (de Nooy *et al.*, 2000). Coupling of the carboxylic group to amines, aldehydes or thiols prior to cross-linking has also been performed with the aim to introduce new functional groups facilitating the cross-linking (Bulpitt & Aeschlimann, 1999; Shu *et al.*, 2002).

Although chemical modifications have focused on the carboxylic acid and the hydroxyl groups, the acetamido group is also a possible target. Initial deacetylation to produce amines is the preferred strategy. Sequentially the amines can be reacted with a cross-linker to form for example amide bonds (Crescenzi *et al.*, 2002).

### 2.2.2 Modified HA for drug delivery

HA is used for controlled or targeted release of drugs and to assist administration of drugs that otherwise can be difficult to introduce *in vivo*. Many of these

applications are still at *in vitro* stage and more research is required before they can be utilised (Huang & Huang, 2018). The active substance can be covalently linked to HA, either directly or by intermediate linkers (Luo *et al.*, 2000b). The active substance can also be physically loaded to a cross-linked hydrogel (Barbucci *et al.*, 2003). HA can be used as a coating of liposomes, nanoparticles or implants (Köwitsch *et al.*, 2018). Often different types of copolymers are added to achieve desired properties. HA can also be the constituent of nanoparticles or microcapsules used for drug-delivery (Fallacara *et al.*, 2018; Köwitsch *et al.*, 2018). For example, HA was modified with glycyrrhetic acid and histidine to produce nanoparticles that could be loaded with doxorubicin, creating a pH-sensitive delivery system for treatment of liver cancer (Tian *et al.*, 2019). HA hydrogels have also been used for topical administration of a variety of drugs (Luo *et al.*, 2000a).

## 2.3 Enzymatic and chemical degradation of HA

The estimated half-life of HA *in vivo* is only about 2-5 min in the blood and about 1-2 days in the skin (Stern, 2004). The regulation of the polymer size and concentration, through *in vivo* synthesis and degradation, is of great importance since different biological effects are attributed to HA of different size. Many enzymes, both eukaryotic and prokaryotic, can cleave HA. Degradation of HA can also be accomplished by various non-enzymatic ways. A comprehensive review on the degradation of HA was given by Stern *et al.* (2007).

### 2.3.1 Hydrolases (EC 3.2.1.-)

Hydrolases cleave bonds through hydrolysis. Glycosidic linkages can be hydrolysed by a double displacement mechanism giving retention of anomeric configuration, or by a direct displacement mechanism resulting in an inversion of anomeric configuration. Human hyaluronidases have been proposed to proceed by the double displacement mechanism (Jedrzejak & Stern, 2005).

Hyaluronoglucosaminidases (EC 3.2.1.35) cleave HA through hydrolysis of the  $\beta(1\rightarrow4)$ -linkages (Figure 4a). The human genome has six hyaluronidase-like sequences, five are active and one is expressed as a pseudogene. Three hyaluronidases are more abundant and their activities are well characterised. Hyaluronidase-2 is situated on the cell membrane and makes the initial cleavage of HA. The fragments from this cleavage (~20 kDa) are then internalised and further degraded by hyaluronidase-1 in the lysosomes (Csoka *et al.*, 2001). PH-20 is referred to as the “sperm” or “testicular” enzyme but is confusingly also present in other tissues than the testis. PH-20 cleaves HA down to

tetrasaccharides and is involved in fertilisation (Hofinger *et al.*, 2007). Hyaluronidase-3 has not yet shown any activity towards HA (Atmuri *et al.*, 2008) and hyaluronidase-4 has proven to be specific towards chondroitin sulphate (CS) (Kaneiwa *et al.*, 2010).

Hyaluronoglucosaminidase is also common in venoms where it serves as a spreading factor by making tissues less viscous around the infection site thus facilitating diffusion of toxic substances from the venom (Kudo & Tu, 2001; Kemparaju & Girish, 2006; Magalhães *et al.*, 2008).

Other hydrolases, which cleave HA through hydrolysis of the  $\beta(1\rightarrow3)$ -linkages instead of the  $\beta(1\rightarrow4)$ -linkages (Figure 4b), are the hyaluronoglucuronidases (EC 3.2.1.36). These enzymes are extracted from leeches (Yuki & Fishman, 1962; Hovingh & Linker, 1999; Yuan *et al.*, 2015).

### 2.3.2 Lyases (EC 4.2.2.-)

GAG lyases are available from a variety of bacterial sources. They are divided into groups depending on their specificity, but many lyases are not so specific and can also cleave other GAGs than what is implied by their names (Linhardt *et al.*, 1986). The lyases discussed here are hyaluronate lyases (EC 4.2.2.1) and chondroitin lyases (EC 4.2.2.4 and EC 4.2.2.5). Common for all lyases of these groups is that they cleave the  $\beta(1\rightarrow4)$ -linkage by a  $\beta$ -elimination reaction, which produces a double bond between C4 and C5 on the uronic acid (Figure 4c). The suggested mechanism is a proton acceptance and donation mechanism (Jedrzejewski, 2000). The symbol  $\Delta$  is used to indicate the presence of unsaturation. For HA and CN, the lytic cleavage results in  $\Delta^{4,5}$ -unsaturated glucuronic acid ( $\Delta$ GlcA) at the non-reducing end (Linhardt *et al.*, 1986).

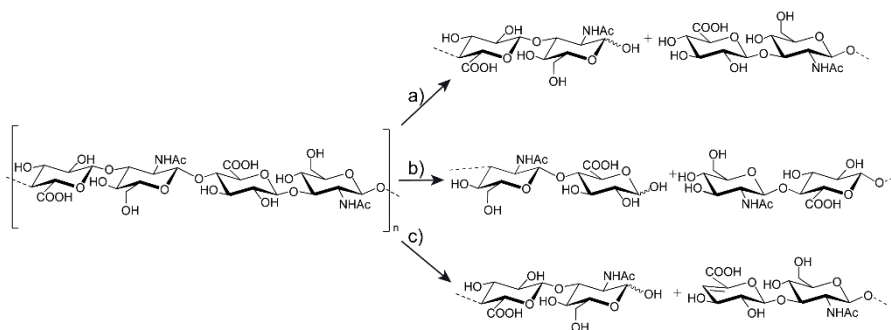


Figure 4. Enzymatic degradation of HA through a) hydrolytic cleavage of the  $\beta(1\rightarrow4)$ -linkage, b) hydrolytic cleavage of the  $\beta(1\rightarrow3)$ -linkage and c) lytic cleavage of the  $\beta(1\rightarrow4)$ -linkage by  $\beta$ -elimination.

### 2.3.3 Non-enzymatic degradation

HA can be depolymerised using both alkaline and acidic hydrolysis. Dilute and semidilute solutions of HA are degraded at pH <4 and >11 with faster degradation occurring at high pH (Maleki *et al.*, 2008). At pH below pK<sub>a</sub> of the uronic acids, hydrolysis mainly occur at the  $\beta(1\rightarrow4)$ -linkage. This type of degradation provides a mixture of mono- and oligosaccharides of different sizes. A  $\beta$ -elimination can also occur instead of hydrolysis and it is common that alkaline or acidic treatment results in “peeling” from the non-reducing end (Kiss, 1974). The random nature of the degradation process makes it hard to control and thus not very useful if site-specific degradation is required.

HA is not very sensitive to thermal degradation but an exponential decrease in viscosity of HA solutions has been observed upon storage at increasing temperatures. At 90 °C, a 10% decrease in viscosity was observed after 1 h (Lowry & Beavers, 1994). HA samples stored at 60-90 °C for 1 h showed only moderate degradation while at 128 °C extensive degradation occurred (Reháková *et al.*, 1994). In a more recent study of HA as both powder and in a solution, only moderate degradation was observed at 37 and 60 °C, while significant degradation was observed at 90 and 120 °C (Mondek *et al.*, 2015).

Several studies have been devoted to the degradation of HA by reactive oxygen and nitrogen species (ROS/RNS). They can result in either specific or non-specific cleavage of the polysaccharides. These types of degradation pathways are often associated with different types of human diseases and conditions. For example, ROS/RNS play important roles in wound healing, and in rheumatic- and osteoarthritis (Li *et al.*, 1997; Moseley *et al.*, 1997). Together with enzymes, radical degradation is the most important process for *in vivo* degradation of HA (Duan & Kasper, 2011).

## 2.4 Analysis of physical and chemical properties of HA-BDDE hydrogels

Even though all HA-BDDE hydrogels are produced from the same building blocks, *i.e.* HA and BDDE, there is a great variety of HA-BDDE hydrogels with different properties. The differences are both measurable from the physical properties, such as rheological parameters, swelling behaviour, particle size and distribution, and from chemical properties, such as molecular weight of HA raw material, amount of modification, amount of cross-linking, substitution positions, and distribution of cross-links.

### Rheological parameters

Hydrogels are highly viscous and viscoelastic materials and thus rheological properties are used for comparison of gel strength. Application of a force to a viscoelastic material will cause irreversible deformation (viscous) and reversible deformation (elastic). Viscoelastic properties can be studied using oscillatory rheology. The applied force is oscillated back and forth, instead of rotated continuously, giving a sinusoidal force curve. Four parameters are often used to describe the viscoelastic properties: i)  $G^*$  - the complex modulus which is the overall resistance of the material to deformation, ii)  $G'$  - the elastic modulus (or storage modulus) which is the transient deformation, iii)  $G''$  - the viscous modulus (or loss modulus) which is the permanent deformation and (iv)  $\delta$  - the phase shift angle.

At low frequencies, concentrated solutions of unmodified HA have a  $G''$  larger than  $G'$  (viscous behaviour). At high frequency,  $G'$  is larger than  $G''$  (elastic behaviour) (Gibbs *et al.*, 1968). This is a typical behaviour for entangled networks, since at low frequency the polysaccharide chains can disentangle and thereby behave viscously, while at high frequency the short time span does not allow for disentanglement, resulting in a seemingly cross-linked gel due to remaining entanglements. For cross-linked HA hydrogels,  $G'$  is always higher than  $G''$ . Strong gels have  $G'$  and  $G''$  values that are essentially frequency independent, while a weaker gels might reveal some frequency dependence (Figure 5) (Barbucci *et al.*, 2003).

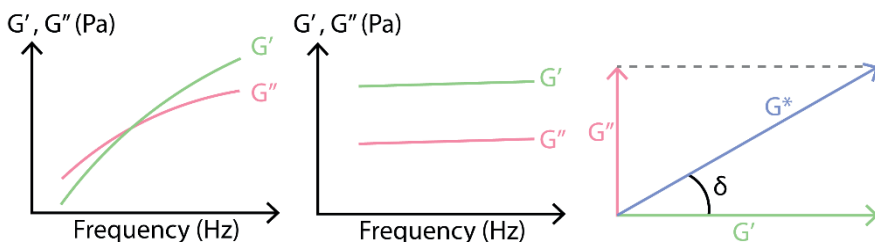


Figure 5. Schematic illustration of theoretical behaviour of a HA solution (left) and a HA hydrogel (middle) during an oscillatory frequency sweep. (Right) relationship between  $G'$ ,  $G''$ ,  $\delta$  and  $G^*$ .

The complex modulus ( $G^*$ ) describes the combined viscoelastic behaviour, it is a vector sum of  $G'$  and  $G''$  (Figure 5). The phase shift angle ( $\delta$ ) shows the lag period between the sinusoidal function of the applied strain and the measured stress. The loss tangent,  $\tan \delta$ , describes the ratio between  $G''$  and  $G'$  (Eq. 1). For liquids,  $\tan \delta > 1$  and for solids and gels  $\tan \delta < 1$  (Barbucci *et al.*, 2000). High  $G'$  and low  $\tan \delta$  are associated with strong hydrogels.

$$\tan \delta = G''/G' \quad (\text{Eq. 1})$$

### *Swelling*

The strength of the gel can also be assessed by measuring its ability to swell. HA solutions will, if infinite solvent is added and sufficient time is allowed, be diluted to infinity. A hydrogel on the other hand will have an endpoint for dilution when fully swollen. A weak gel will swell more than a strong gel. A swelling factor describes the ratio between volume of a fully swollen gel and initial volume of the gel and thus depend on the initial concentration of the gel. Alternatively, the swelling degree is a measurement of the ratio between the weight of the dried hydrogel to that of the fully swollen hydrogel (Barbucci *et al.*, 2000). The lowest possible concentration of the gel phase at equilibrium ( $c_{min}$ ) can be calculated from the swelling factor, HA concentration and gel content (Edsman *et al.*, 2012). The swelling behaviour of hydrogels depend on the swelling medium and on the temperature. Sufficient time has to be allowed to reach equilibrium.

### *Gel content - extractable HA*

Cross-linked HA hydrogels often contain HA chains that are not connected to the cross-linked network. This amount can be determined by washing out the unbound portion and quantifying it. Shaking the cross-linked hydrogel in an excess of solvent will cause the gel to swell and allow the unbound chains to diffuse out from the cross-linked network. The extractable HA can then be filtered off and the HA content can be quantified by the carbazole method (Dische & Rothschild, 1967; Knutson & Jeanes, 1968). The gel content, which can later be calculated, refers to the portion of HA that is part of the cross-linked network and thus could not be extracted (Edsman *et al.*, 2012).

### *Particle size and distribution*

The cross-linking of HA with BDDE results in one giant molecule. The hydrogel has to be downsized into smaller hydrogel pieces to enable administration through injection. This is often achieved by pressing the hydrogel through sieves with holes of desired size or by homogenisation (Tezel & Fredrickson, 2008). The resulting product thereby consists of HA hydrogel particles. The soft and transparent nature of the particles makes them appear as one continuous material (Kablik *et al.*, 2009; Öhrlund & Edsman, 2015). The particle size distribution in the hydrogels can be analysed using a particle analyser (Kablik *et al.*, 2009) or microscopic techniques such as scanning electron microscopy (SEM) (Park *et al.*, 2013).

### *Degree of modification and degree of cross-linking*

Several parameters are used to describe the degree of cross-linking and modification in HA (Table 1). Analysis of the degree of modification (MoD) by  $^1\text{H}$  NMR spectroscopy and effective cross-linker ratio (CrR) by liquid chromatography- mass spectrometry (LC-MS) was described by Kenne *et al.* for HA-BDDE hydrogels (Kenne *et al.*, 2013). An alternative approach used alkaline degradation instead of enzymatic degradation before  $^1\text{H}$  NMR analysis for MoD and size exclusion chromatography (SEC) analysis for degree of cross-linking (CrD) (Guarise *et al.*, 2012). FT-IR has been used to assess the degree of cross-linking by correlation to loss of hydroxyl signals (Al-Sibani *et al.*, 2017). For HA hydrogels cross-linked at the carboxylic acid,  $^1\text{H}$  NMR has been used to determine the degree of substitution (Shu *et al.*, 2002) and  $^{13}\text{C}$  NMR for determination of the cross-linking degree (Barbucci *et al.*, 2006).

*Table 1.* Definitions, abbreviations and equations for some parameters used to describe modification and cross-linking of hydrogels (Kenne *et al.*, 2013).

<b>Parameter</b>	<b>Abb.</b>	<b>Description</b>	<b>Equation</b>
Degree of modification	MoD	Ratio of moles of cross-linkers ( $n_X$ ) to moles of repeating unit ( $n_R$ )	$MoD = \frac{n_X}{n_R}$
Degree of substitution	DS	Ratio of moles of substituted repeating units ( $n_{R-X}$ ) to moles of repeating unit ( $n_R$ )	$DS = \frac{n_{R-X}}{n_R}$
Effective cross-linker ratio	CrR	Ratio of moles of double-linked cross-linker ( $n_{X(-R)_2}$ ) to moles of cross-linker ( $n_X$ )	$CrR = \frac{n_{X(-R)_2}}{n_X}$
Degree of cross-linking	CrD	Ratio of moles of double-linked cross-linker ( $n_{X(-R)_2}$ ) to moles of repeating unit ( $n_R$ )	$CrD = \frac{n_{X(-R)_2}}{n_R}$
Degree of cross-linking	DC	Ratio of moles of cross-linked repeating units ( $n_{R-X-R}$ ) to moles of repeating unit ( $n_R$ )	$DC = \frac{n_{R-X-R}}{n_R}$

It is important to define clearly what has been measured when reporting data. For instance, degree of modification (MoD) and degree of substitution (DS) describe essentially the same thing but in different ways. MoD measures the number of cross-linkers in relation to the number of disaccharides while DS measures the number of substituted disaccharides in relation to the total number of disaccharides. A hydrogel consisting of ten repeating units (R) and four cross-linkers (X), two double-linked and two mono-linked, will thus have a MoD of 40% (4/10) and a DS of 60% (6/10) (Figure 6).

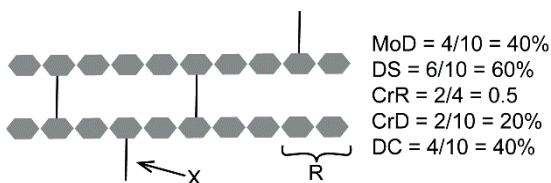


Figure 6. Schematic illustration of a cross-linked hydrogel exemplifying the parameters described in Table 1. R – repeating unit of the polysaccharide, X – cross-linker.

The degree of modification and degree of cross-linking affect the physicochemical properties of the hydrogels. Generally, more efficient cross-linking will produce hydrogels with higher gel strength (high  $G^*$ , low  $\tan \delta$  and high  $c_{min}$ ). The differences in physical properties of hydrogels can be explained to some extent by the chemical parameters discussed above. However, the positions of substitution and the cross-link distribution might also affect the physical properties of the hydrogel. Substitution of the carboxylic acid, if extensive, affects the anionic character of HA. For modification of the hydroxyl groups, there are four possible substitution positions that might have different effect (Figure 1). The cross-link distribution might be even, random or block-wise. Chain-loops and other configurations that do not contribute to gel strength may also occur (Borzacchiello & Ambrosio, 2009). The cross-link distribution or porosity has been assessed in other hydrogels by calculating “mesh size” ( $\zeta$ ) or molecular weight between cross-links ( $M_c$ ) which are both calculated from the elastic modulus ( $G'$ ) (Oommen *et al.*, 2013).

### 3 Chondroitin

Chondroitin sulphate (CS) is a GAG that has a primary structure very similar to that of HA. Disregarding sulphation, their structure differ only by the orientation of the hydroxyl at position four of the aminoglycan. The repeating unit of desulphated chondroitin (CN) is thus  $\rightarrow 4$ )- $\beta$ -D-GlcA-(1 $\rightarrow$ 3)- $\beta$ -D-GalNAc-(1 $\rightarrow$  (Figure 7). HA is the only naturally occurring non-sulphated GAG but by desulphation of CS, production of CN is possible (Takano, 2002). The molecular weight of CS is generally much lower than that of HA (< 50 kDa). CS often occurs as a proteoglycan, *i.e.* attached to a protein (Köwitsch *et al.*, 2018).

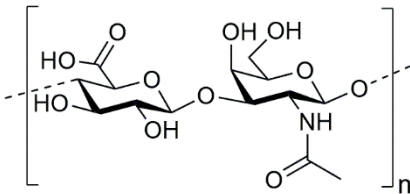


Figure 7. Repeating unit of desulphated chondroitin  $\rightarrow 4$ )- $\beta$ -D-GlcA-(1 $\rightarrow$ 3)- $\beta$ -D-GalNAc-(1 $\rightarrow$ .

## 4 Methods

### 4.1 NMR Spectroscopy

#### 4.1.1 Principle

Nuclear magnetic resonance (NMR) spectroscopy has since the discovery of proton magnetic resonance in 1946 grown to become one of the most important analytical techniques in chemistry. Bloch *et al.* published a short note about their successful results almost simultaneously as Purcell *et al.* (Bloch *et al.*, 1946; Purcell *et al.*, 1946). Only a few years later (1952), the importance of their discoveries was acknowledged when they were jointly awarded the Nobel Prize in physics (Bloch, 1953; Purcell, 1953). Many improvements have since then contributed to make NMR the useful tool that it is today (Emsley & Feeney, 1995; Emsley & Feeney, 2007).

All nuclei that have a nuclear spin quantum number ( $I$ ) larger than zero can be observed by NMR. The nuclear spin quantum number is an intrinsic property of the nucleus. It is a multiple of  $\frac{1}{2}$  and it can be larger than or equal to zero. All nuclei carry a charge and if they are spinning, they will possess a magnetic moment ( $\mu$ ). Placing nuclei in a strong static magnetic field ( $B_0$ ) will cause the microscopic magnetic moments of each nucleus to align in the direction of the field in a discrete number of directions (Figure 8).

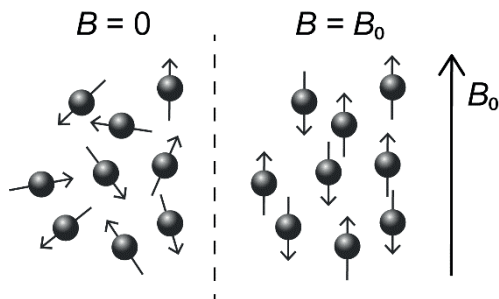


Figure 8. In a strong static magnetic field ( $B_0$ ) nuclear spins with  $I = \frac{1}{2}$  will align parallel or antiparallel to  $B_0$ .

One of the most utilised nuclei is the hydrogen isotope  $^1\text{H}$ , which has a nuclear spin quantum number  $I = \frac{1}{2}$  and a high natural abundance (99.98%). A nucleus of nuclear spin quantum number  $I$  has  $2I + 1$  spin states. For  $^1\text{H}$ , two separate spin states are thus possible,  $+\frac{1}{2}$  and  $-\frac{1}{2}$  often referred to as  $\alpha$  and  $\beta$ . At equilibrium, there is a population difference between  $\alpha$  and  $\beta$  spin states, which is predicted by the Boltzmann distribution from the energy difference between the two spin states. This population difference gives rise to a net magnetisation along the axis of the static magnetic field (referred to as the z-axis). The magnetic moments are actually not aligned with the z-axis, but rather precessing around the z-axis at a frequency known as the Larmor frequency. The net magnetization can then be perturbed by adding another weaker magnetic field perpendicular to the static one. This is achieved by applying radiofrequency (RF) pulses corresponding to the energy difference between the spin states causing transitions to occur (resonance). Structural information can be obtained by manipulating spins using different types of pulse sequences. Pulse sequences consist of different combinations of RF pulses and delays and are ended by an acquisition time when the signal caused by perturbation of the net magnetisation is recorded.

The signal observed by NMR is called the free induction decay (FID). It is the alternating current induced in the receiver coil by the transverse component of the bulk magnetisation precessing at the Larmor frequency as it is returning to equilibrium. All information accessible from a NMR spectrum is included in the FID but interpretation of the data in this form is difficult. Fourier transformation of the FID is utilised to transform the data from the time domain to the frequency domain (Figure 9).

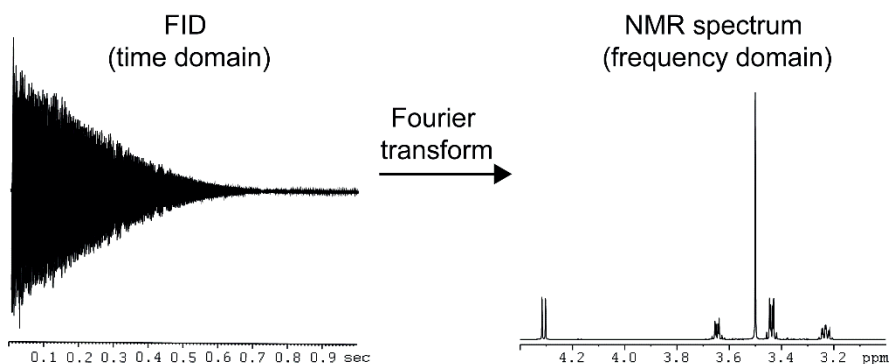


Figure 9. The free induction decay is collected in the time domain and converted to the frequency domain by Fourier transformation. 1D  $^1\text{H}$  NMR of Me- $\beta$ -GlcA in  $\text{D}_2\text{O}$  at 25  $^\circ\text{C}$ .

The local magnetic field is the field that a particular nucleus experiences. Electrons surrounding the nucleus shield it from the  $B_0$  field reducing the local magnetic field. Due to differences in chemical environment, the electronic distribution around nuclei will vary, and thus their local magnetic field will vary. These variations cause the nuclei to resonate at slightly different frequencies. The frequency deviation from a standard nucleus is measured as the chemical shift ( $\delta$ ). Frequencies are measured in Hz but for convenience  $\delta$  values are converted to parts per million (ppm).

Indirect interactions between nuclear spins through covalent bonds are called scalar couplings (or  $J$ -couplings). For a nucleus with two spin states, one of the spins will cause a slight increase in the frequency of the coupled nuclei while the other will cause a slight decrease. This will thus cause a splitting of the signal into two peaks (a doublet) at  $\delta+J/2$  and  $\delta-J/2$ . Coupling to more than one nuclear spin produces higher order coupling patterns (*i.e.* triplets, quartets, doublet of doublets).  $J$ -coupling constants are reported in Hz and are often observed over one ( $^1J$ ), two ( $^2J$ ) or three ( $^3J$ ) bonds.  $J$ -couplings can provide insight into connectivity, bond distances and angles.

Nuclei can affect each other not only through covalent bonds but also through space by dipolar couplings. The local magnetic field of each nucleus will affect the relaxation of other nuclei that are sufficiently close in space. This type of cross-relaxation is referred to as the nuclear Overhauser effect (NOE). The NOE is detected as the change in intensity of a spin upon perturbation (saturation or inversion) of a coupling spin. The change in intensity by NOE can be either positive or negative. For elucidation of conformations, the NOE is very useful since it is related to the distance between nuclei through space (Shapiro, 2011).

### 4.1.2 Relaxation

The process by which spins return to equilibrium after applying RF pulses is called relaxation. The relaxation time determines how fast the excitation can be repeated without saturating the spins. It can provide useful insights into molecular conformations and dynamics. The relaxation is described by two different processes: i) longitudinal (or spin-lattice) relaxation ( $T_1$ ) and ii) transverse (or spin-spin) relaxation ( $T_2$ ).

Restoration of the magnetisation in the z-direction through energy transfer to neighbouring molecules (the lattice), in the form of vibrational and rotational energy, is defined as longitudinal relaxation ( $T_1$ ). For energy transfer to be possible, fluctuating magnetic fields are required, which can be caused by a number of sources. One constantly present source is the dipole-dipole interaction. In solutions, molecular motions will cause fast reorientation of dipole interactions leading to fluctuating magnetic fields. Since temperature affects the rate of molecular motions,  $T_1$  is also temperature dependent. Paramagnetic substances such as molecular oxygen are other sources of longitudinal relaxation. If the nuclei of a molecule have very long relaxation times, the addition of a small amount of a paramagnetic species can give more efficient relaxation.  $T_1$  is often relatively long (milliseconds – seconds) for small molecules in solution.  $T_1$  governs the rate at which an experiment can be repeated.

The second process of relaxation is the transverse relaxation, which is the loss of coherent magnetisation in the xy-plane. The same mechanisms that cause  $T_1$  relaxation also cause  $T_2$  relaxation, but  $T_2$  relaxation can also be induced by other processes resulting in  $T_2$  always being equal to or shorter than  $T_1$ . For example, inhomogeneity of the magnetic field will contribute to  $T_2$  relaxation since nuclear spins will experience slightly different local magnetic fields. Chemical exchange will also contribute to  $T_2$ . The transfer of a nucleus from one chemical environment to another is referred to as chemical exchange.

### 4.1.3 NMR for studies of carbohydrates

NMR spectroscopy is an important tool for analysis of structure, conformation and dynamics of carbohydrates. The structural differences between carbohydrates are often small, sometimes only the orientation of one bond discerns two carbohydrates from each other. NMR spectroscopy is one of few analytical techniques that enables differentiation between these isomers. Information about ring connectivities, anomeric configuration and sites of modifications on sugars can also be obtained by NMR spectroscopy.

The nucleus most commonly used for studies of carbohydrates by NMR spectroscopy is proton ( $^1\text{H}$ ). Because the intensity of the NMR signal is directly proportional to the number of nuclei contributing to the signal, one-dimensional (1D)  $^1\text{H}$  NMR is widely used for quantification purposes. Specific signals representative of a particular molecule or of part of it, which are located in a well resolved part of the NMR spectrum can be used for identification or quantification and are referred to as “structural-reporter-resonances” (Vliegthart *et al.*, 1983). One limitation of  $^1\text{H}$  NMR as a tool for quantification is overlapping signals. For carbohydrates, proton signals in the anomeric region (4.4-5.5 ppm) are generally well resolved, while the other ring protons are located in a narrow region (3-4.2 ppm) and usually suffer from signal overlap (Duus *et al.*, 2000).

Carbon NMR is also widely used in structural studies of carbohydrates, but the most abundant isotope,  $^{12}\text{C}$  (98.9% abundance), has a spin quantum number of zero and is thereby NMR silent. Instead, the isotope  $^{13}\text{C}$  (1.1% abundance) is used, making  $^{13}\text{C}$  NMR much less sensitive compared to  $^1\text{H}$  NMR. One advantage of  $^{13}\text{C}$  NMR is the much broader range of chemical shifts in comparison to  $^1\text{H}$ , making signal overlap often less critical. In order to use 1D  $^{13}\text{C}$  NMR as a quantitative tool some considerations have to be taken (Freeman, 1972). First, interpretation of  $^{13}\text{C}$  NMR spectra can be difficult due to the splitting of  $^{13}\text{C}$  signals from coupling to  $^1\text{H}$ . In addition, to avoid loss of sensitivity due to peak splitting, broadband decoupling of  $^1\text{H}$  resonances is often used in  $^{13}\text{C}$  NMR experiments. Without decoupling, a  $^{13}\text{C}$  spectrum with coupling and without NOE enhancement is obtained.

Decoupling of the proton signals prior to data acquisition produces a NMR spectrum with both coupling and NOE enhancement (gated decoupling experiment, Figure 10a). By decoupling of the proton signals during acquisition, a spectrum with neither coupling nor NOE enhancement is produced (inverse gated decoupling, Figure 10b). If both decoupling and NOE enhancement are desired, decoupling is applied throughout the whole experiment, (power gated decoupling, Figure 10c). For quantitative  $^{13}\text{C}$  NMR, the NOE should be eliminated by using an inverse-gated decoupling sequence. Longer experimental time is required to reach the same signal-to-noise ratio as in power gated decoupling experiments. The experimental time is also prolonged since the relaxation delay should be a minimum of  $5xT_1$  (Mareci & Scott, 1977).

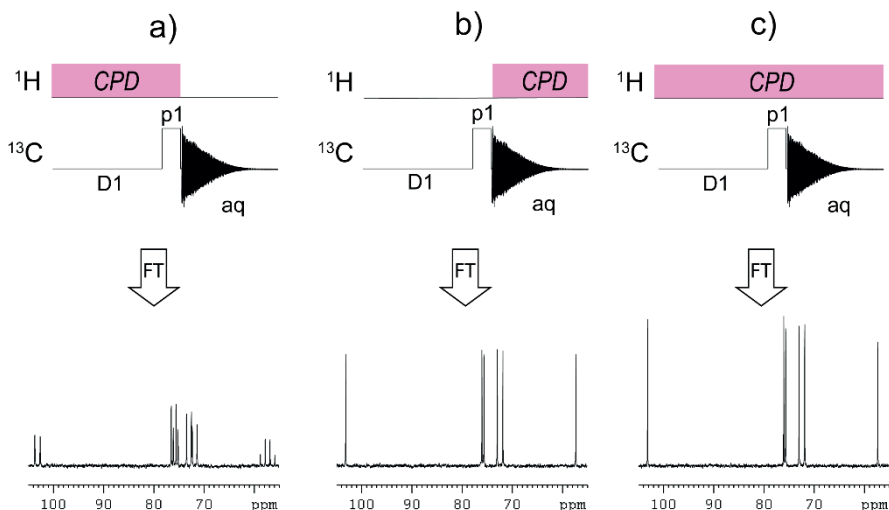


Figure 10. 1D  $^{13}\text{C}$  NMR with composite pulse decoupling (CPD) a) prior to acquisition – gated decoupling, b) during acquisition – inverse gated decoupling or c) continuously – power gated decoupling. Sample: Me- $\beta$ -GlcA in  $\text{D}_2\text{O}$ . CPD scheme: Waltz-16 (Shaka *et al.*, 1983).

Structural analysis of carbohydrates is usually conducted using a combination of  $^1\text{H}$ - $^1\text{H}$  homonuclear (COSY, TOCSY, NOESY) and  $^1\text{H}$ - $^{13}\text{C}$  heteronuclear (HSQC, HMBC) 2D NMR experiments. The COSY (correlation spectroscopy) spectrum shows correlation through scalar coupling between adjacent protons, whereas the TOCSY (total correlation spectroscopy) spectrum shows correlations between all of the coupled protons in a spin system. The NOESY (nuclear Overhauser effect spectroscopy) experiment shows correlations through space (Figure 11).

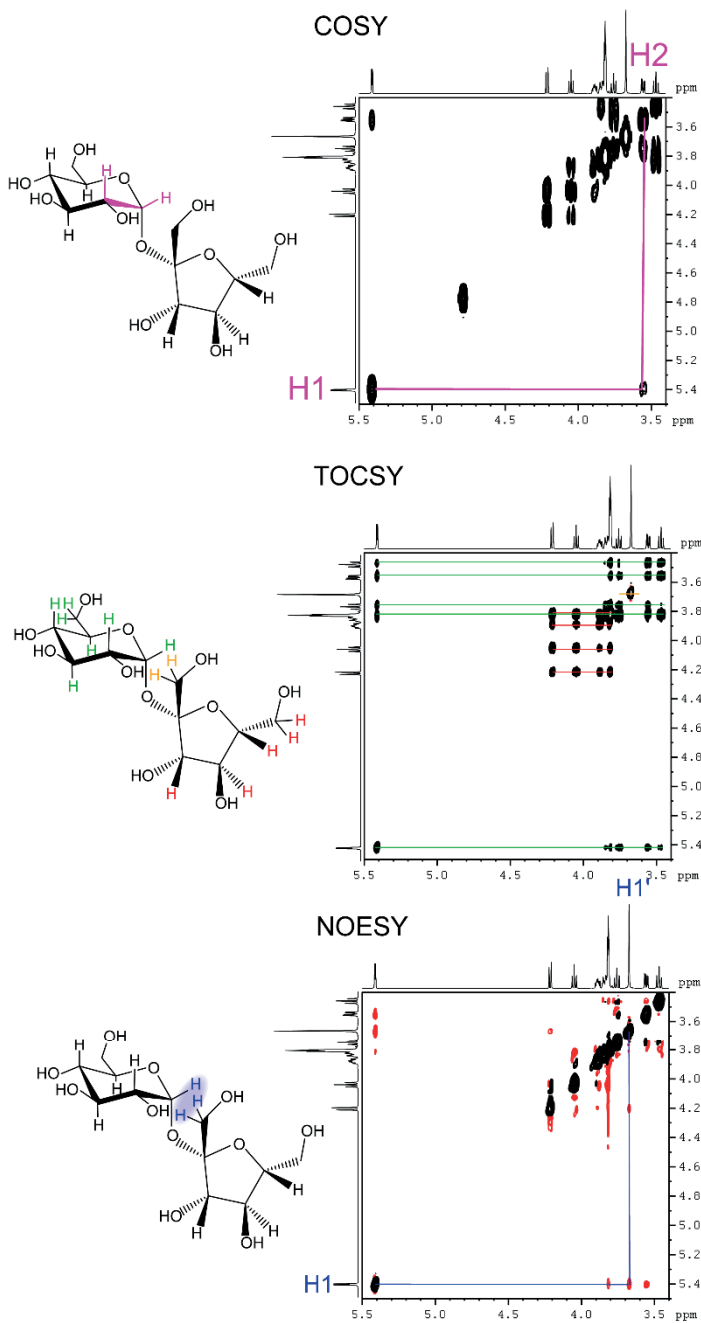


Figure 11. 2D homonuclear NMR spectra of sucrose in D<sub>2</sub>O providing information about i) neighbouring nucleus (COSY), ii) spin systems (TOCSY) and iii) proximity through space (NOESY).

The heteronuclear single quantum correlation (HSQC) experiment provides correlations between proton and carbon connected by one covalent bond (*i.e.* H-C). The HSQC and TOCSY sequences can be combined into a 2D HSQC-TOCSY (Figure 12). In this experiment, correlations are obtained between all coupled protons in a spin system and each carbon that connects directly to a proton in that spin system. This is especially useful when overlap in the proton spectrum prevents analysis since often the corresponding carbons are better resolved. In carbohydrate analysis, each monosaccharide unit will be one separate spin system.

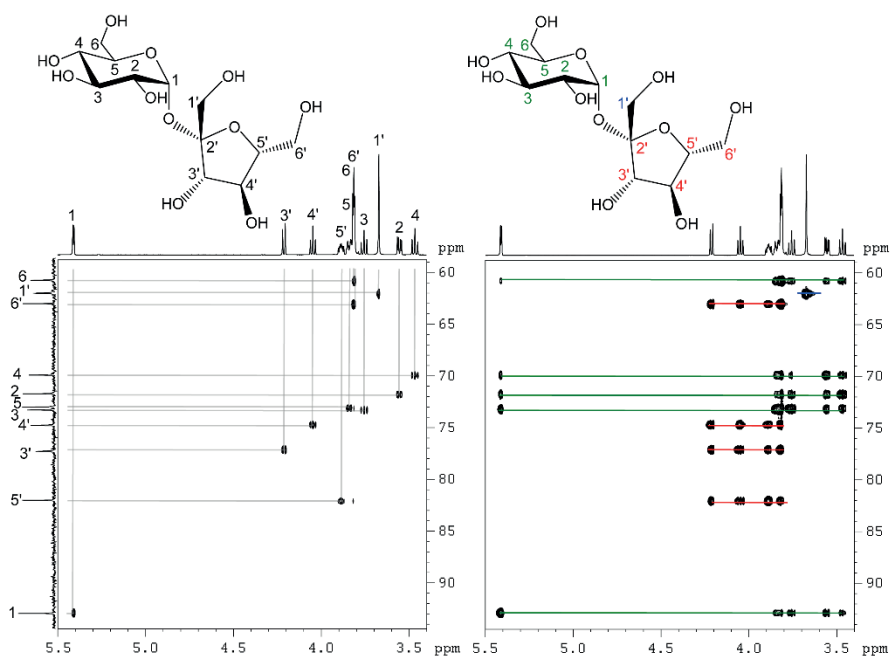


Figure 12. 2D heteronuclear NMR spectra of sucrose in D<sub>2</sub>O. HSQC (left) and HSQC-TOCSY (right).

Quaternary carbons are not observed from HSQC or HSQC-TOCSY experiments, because they do not connect directly to protons. Long-range couplings (2-3 bonds) between protons and carbons can be observed using a heteronuclear multiple bond correlation (HMBC) experiment. In carbohydrate chemistry, this experiment is important for determination of ring connectivities (Figure 13).

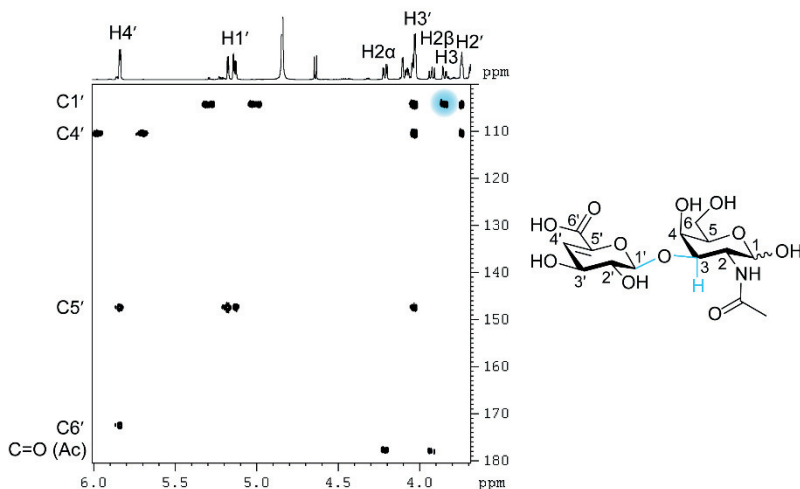


Figure 13.  $^1\text{H}$ - $^{13}\text{C}$  HMBC spectrum of unsaturated desulphated chondroitin disaccharide ( $\Delta\text{CN}_2\text{-B}$ ). The ring connectivity can be obtained from the 3-bond coupling over the glycosidic linkage ( $\text{C}1'$  to  $\text{H}3$ ). Couplings to quaternary carbons allow for determination of  $\delta^{13\text{C}}$  of  $\text{C}6'$ ,  $\text{C}5'$  and the carbonyl carbon of the acetamido group.

#### 4.1.4 Exchangeable protons

Hydroxy, amide and amine protons are referred to as exchangeable protons since they easily exchange with protons from the solvent. To be able to analyse these protons, either aprotic solvents (solvents with no exchangeable protons *e.g.* DMSO, acetone- $d_6$ ) or non-deuterated protic solvents are required. When non-deuterated protic solvents (*e.g.*  $\text{H}_2\text{O}$ ) are used, the signal from the solvent will be dominating and need to be suppressed. The pH and temperature should be adjusted to reduce the chemical exchange between exchangeable protons of the sample and of the solvent (Liepinsh *et al.*, 1992). If the exchange is too fast the signal of the hydroxyl protons will coalesce with the water proton signal (Figure 14).

Measuring the chemical shift difference between the hydroxy protons of an oligo- or polysaccharide in comparison with the corresponding monosaccharide ( $\Delta\delta^{\text{OH}} = \delta_{\text{poly}} - \delta_{\text{mono}}$ ) can provide information about hydration and hydrogen bonding. Upfield shift indicates hydrogen bonding to a neighbouring ring oxygen or steric hindrance from bulk water while a downfield shift has been attributed to hydrogen bonding with another hydroxyl group (Sandström *et al.*, 1998; Ivarsson *et al.*, 2000; Bekiroglu *et al.*, 2004). Hydroxyl protons involved in hydrogen bonding will be less affected by temperature changes than those that are not due to reduced interactions with the solvent. Measuring the temperature coefficients ( $d\delta/dT$ ) can thus also contribute to deducing hydrogen bonding. For

strong hydrogen bonds low temperature coefficients ( $|d\delta/dT| < 3$  ppb/ $^{\circ}\text{C}$ ) have been reported. Hydroxy protons with  $|d\delta/dT| < 11$  ppb/ $^{\circ}\text{C}$  are considered partially hydrated (may participate in transient hydrogen bonding) and hydroxy protons with  $|d\delta/dT| > 11$  ppb/ $^{\circ}\text{C}$  are considered to be fully hydrated (Poppe *et al.*, 1992; Blundell *et al.*, 2006a).

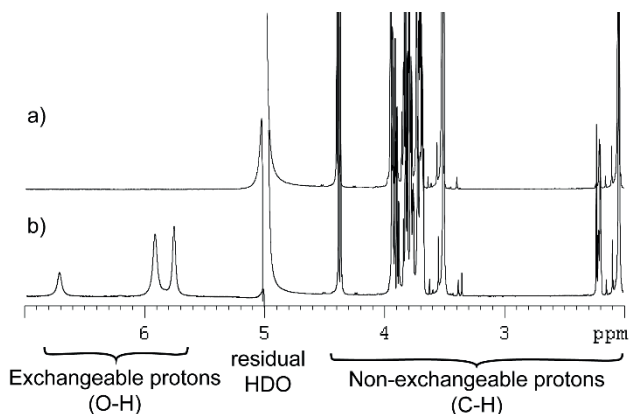


Figure 14. 1D  $^1\text{H}$  NMR spectra of Me- $\beta$ -GalNAc in  $\text{H}_2\text{O}$ :acetone- $d_6$  (85:15) before (a) and after (b) pH adjustment. Recorded at 5  $^{\circ}\text{C}$  with water suppression.

#### 4.1.5 Non-uniform sampling

The traditional way to perform 2D NMR spectroscopy is to record data with linear increment of the evolution time, giving rise to the second dimension. To receive high resolution in the indirect dimension, data must be sampled with enough increments. This can become very time consuming for 2D and higher dimensions NMR experiments.

Non-uniform sampling (NUS) is a method for data acquisition that collects only a fraction of the increments that would usually be collected (Figure 15). The sampling can be radial, follow weighted schemes or be completely random (Kazimierczuk & Orekhov, 2015). Additionally, there are several different methods to reconstruct the spectrum. The choice of sampling schedule and processing technique are both of importance, the optimum choice depend on the research question (Hyberts *et al.*, 2014; Mobli & Hoch, 2014).

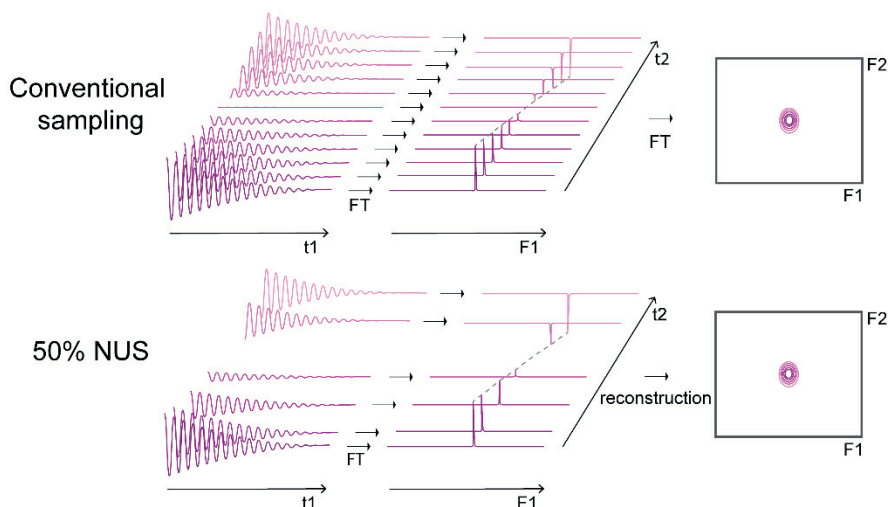


Figure 15. In 2D NMR, using conventional sampling one FID is collected for each increment of the evolution time. In non-uniform sampling (NUS) only a fraction of the FIDs are collected. The remaining FIDs are reconstructed by different processing techniques.

The advantage of NUS is either higher resolution or shorter experiment time. If 20% of the increments are sampled the experiment takes only a fifth of the time, still providing the same resolution (Figure 16). NUS can also be used to improve signal-to-noise ratio or sensitivity (Hyberts *et al.*, 2013; Zambrello *et al.*, 2018).

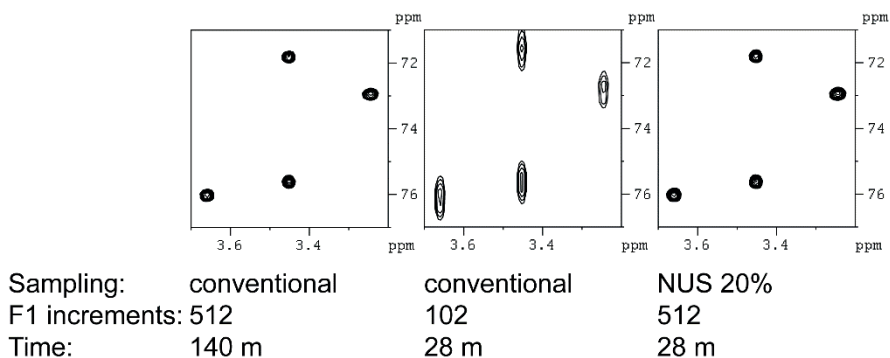


Figure 16. Part of the  $^1\text{H}$ - $^{13}\text{C}$  HSQC NMR spectra of Me- $\beta$ -GlcA obtained using non-uniform or conventional sampling.

## 4.1.6 Determination of relaxation parameters

### *T<sub>1</sub> measurements*

The standard way of measuring  $T_1$  is the inversion recovery experiment (Figure 17). A  $180^\circ$  pulse causes inversion of the magnetisation so that it is aligned along the  $-z$ -axis. During a delay  $\tau$ , longitudinal relaxation is allowed to take place and finally a  $90^\circ$  pulse is applied after which the FID is recorded.

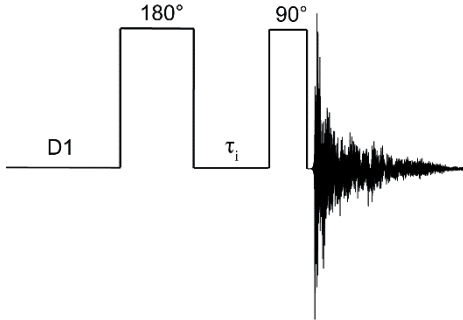


Figure 17. Inversion recovery pulse sequence.

The pulse sequence is repeated with increasing value of  $\tau$ . The peak integral follows an exponential function according to Equation 2 that allows for determination of  $T_1$ .

$$I = I_0 \cdot (1 - 2e^{-\tau/T_1}) \quad (\text{Eq. 2})$$

The inversion recovery experiment might not always be suitable when radiation damping (Bloembergen & Pound, 1954) is significant. An alternative approach is to use the saturation recovery experiment, in which a selective saturation pulse is applied to the signal of interest (Taylor & Peterson, 2010; Krishnan & Murali, 2013). After saturation, relaxation is allowed during a delay  $\tau$  followed by a  $90^\circ$  pulse and recording of FID (Figure 18).

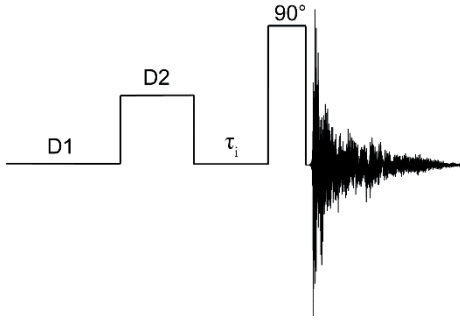


Figure 18. Saturation recovery pulse sequence.

The saturation recovery experiment provides a similar curve as the inversion recovery experiment, but starting from zero following the slightly altered Equation 3.

$$I = I_0 \cdot (1 - e^{-\tau/T_1}) \quad (\text{Eq. 3})$$

### *T<sub>2</sub> measurements*

Transverse relaxation ( $T_2$ ) can be measured by a spin echo experiment. The Carr-Purcell-Meiboom-Gill (CPMG) sequence (Figure 19) uses a  $90^\circ$  pulse to transfer the magnetisation into the  $xy$ -plane followed by a train of spin echoes:  $(\tau-180^\circ-\tau)_n$  where  $\tau$  is a short delay and the number of repeats ( $n$ ) determines the total spin echo time. During the first delay, the magnetisation vectors spread out in the  $xy$ -plane as some spins precess faster and others slower. The  $180^\circ$  pulse pushes the net magnetisation towards the  $-y$ -axis and the second  $\tau$  delay will allow for refocusing of the signal. Some of the net magnetisation is though lost after the spin echo due to transverse relaxation and by recording a series of CPMG experiments with increasing total spin echo time, the  $T_2$  relaxation times can be calculated from Equation 4. CPMG experiments can also be used for filtering of signals with fast  $T_2$  relaxation.

$$I(t) = P \cdot e^{-(t/T_2)} \quad (\text{Eq. 4})$$

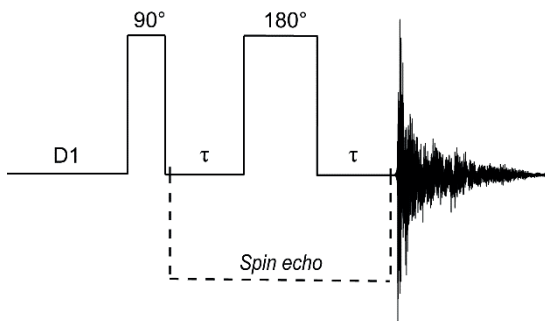


Figure 19. Carr-Purcell-Meiboom-Gill (CPMG) pulse sequence.

#### 4.1.7 Diffusion NMR spectroscopy

Molecular diffusion can be influenced by many physicochemical properties of the sample such as molecular weight, shape, temperature, pH *etc.* Studying the diffusion behaviour of molecules can thus provide insights on these properties. The diffusion coefficient can be measured by using a pulsed gradient spin-echo (PGSE) experiment (Figure 20). A pair of gradients with the same duration and amplitude are used, where the first gradient introduces a spatial label to the molecules. After a delay for diffusion ( $\Delta$ ) and a  $180^\circ$  pulse, the second gradient will refocus spins, but spins that have moved a long distance will be less refocused than spins that have moved a short distance (Johnson, 1999). A series of experiments with increasing gradient strength is used to determine diffusion coefficients ( $D$ ) from the decay of signal with higher gradient strength. A fast decay indicates rapid diffusion and a slow decay indicates slow diffusion.

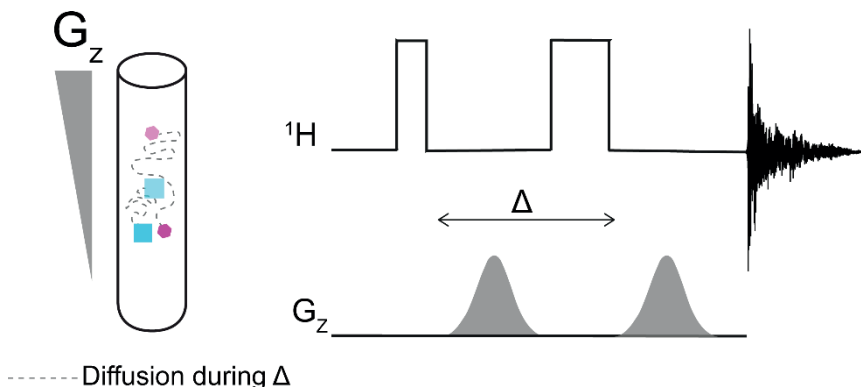


Figure 20. By using gradients in a spin echo, signals of molecules that diffuse slowly will be better refocused compared to molecules with fast diffusion.

Since small molecules diffuse faster than larger molecules, diffusion-edited NMR experiments can be utilised for filtering off signals from small molecules (Figure 21).

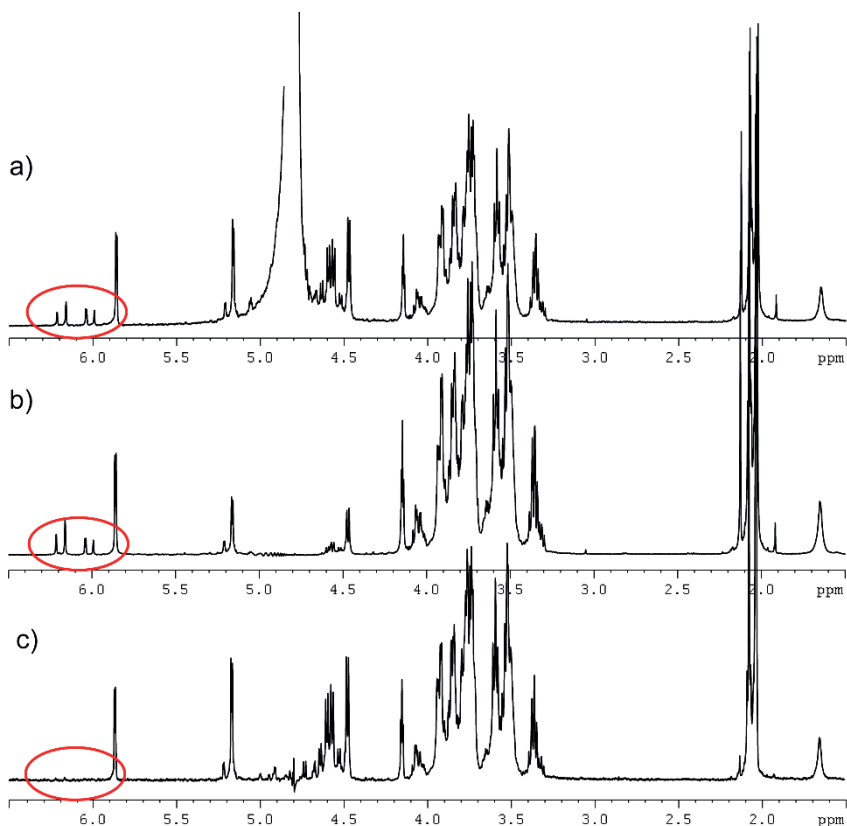


Figure 21. a) 1D  $^1\text{H}$  NMR spectra of  $\Delta\text{HA}_4\text{-B-}\Delta\text{HA}_4$ . H1 and H3 of peeling product, (E)-3-dehydro-en-D-GlcNAc, are circled in red (see Paper II and section 6.1.4 for further explanation) b) 1D  $^1\text{H}$  NMR spectrum with excitation sculpting for water suppression causes attenuation of signals close to the HDO signal c) 1D  $^1\text{H}$  NMR spectrum using a PGSE sequence with bipolar pulse pairs and longitudinal-eddy-current delay (Wu *et al.*, 1995). The signals from the peeling product are filtered off along with the HDO signal.

## 4.2 Mass Spectrometry

Mass spectrometry (MS) is another powerful method for structural investigations. For many compounds MS is a highly sensitive technique requiring very small sample amounts.

In a mass spectrometer, sample molecules are ionised in an ion source. The ions formed are then separated in a mass analyser according to their mass to charge ratio ( $m/z$ ). The  $m/z$ -separated ions are transported to a detector that yields an electric signal proportional to the ion abundance at each  $m/z$  value. The outcome is a mass spectrum with  $m/z$  on the x-axis and the relative ion abundance on the y-axis. The ion corresponding to the original molecule is called the molecular ion. The molecular ion is sometimes fragmented in the mass spectrometer whereby also  $m/z$ -values of the fragment ions can be analysed (MS/MS). In order to distinguish between different ions with similar masses a high mass accuracy and high mass resolution are required. There are several different types of ion sources and mass analysers, and all have their strengths and weaknesses making them suitable for different types of samples.

One benefit of MS is the possibility of connecting it to other analytical techniques such as gas chromatography (GC) and liquid chromatography (LC). When using chromatographic separation directly coupled with MS, sometimes also a detector measuring UV absorption is coupled in serial with the mass spectrometer. Such a system can provide both a UV chromatogram and ion chromatograms, which are generated by plotting the abundance of ions of selected  $m/z$ -values or all ions detected in the mass spectrometer versus the retention time (Figure 22).

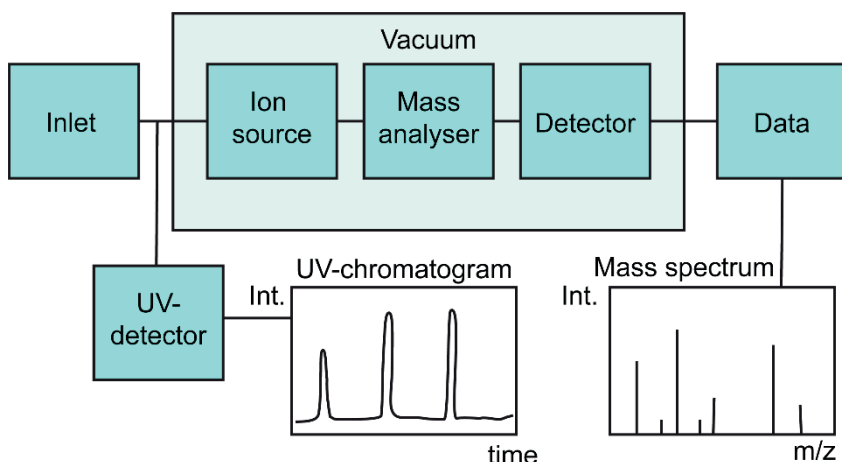


Figure 22. Schematic representation of a mass spectrometer.

#### 4.2.1 Ionisation

The first challenge in MS is to transform the sample molecules into gas phase ions. Depending on the volatility of the sample, this can be achieved in different ways. For volatile compounds, MS can be coupled with GC. In this case, the sample is already in the gas phase and need only to be ionised. The ionisation can be achieved relatively easy by either electron ionisation (EI) (Bleakney, 1929) or chemical ionisation (CI) (Munson & Field, 1966). In an EI ion source, the analyte molecules are exposed to a beam of energetic electrons and when an electron collides with an analyte molecule, an electron is removed from the molecule producing a positive molecular ion (a radical cation  $M^+$ ). EI provides a “hard” ionisation giving a lot of fragmentation of the molecular ion and therefore the resulting mass spectrum can be dominated by signals resulting from detected fragment ions. In CI, a reagent gas (*e.g.* methane) is ionised with the same principle as in EI. The methane ions interact with analyte molecules and through proton transfer, charge transfer or adduct formation the analyte is ionised. CI is a “softer” ionisation technique than EI and induces limited fragmentation and therefore the mass spectrum is dominated by the signal from the molecular ion.

For non-volatile samples, MS is often coupled with liquid chromatography. Large amounts of solvent must then be removed in order to transfer the analytes into the gas phase. Part of the challenge is that vacuum is required in all mass analysers while liquid chromatography is performed at atmospheric pressure. In electrospray ionisation (ESI) (Fenn *et al.*, 1989), the effluent from the liquid chromatography is directly sent through the electrospray – a capillary tube placed in an electric field. The droplets formed by the electrospray will thus be charged. The charged droplets are guided by an electric field into a heated region with successively decreasing pressure, which support evaporation of the droplets. As the droplets become smaller, their surface charge density increases, and when it reaches the Rayleigh limit droplets can subdivide into smaller droplets. The final ion formation is assumed either to occur via ion desorption from a droplet surface or by evaporation of all of the solvent from a droplet that contains an individual ion (Nguyen & Fenn, 2007). Ions formed by ESI are – depending on the electrospray polarity and the system analysed – protonated (or deprotonated) or cation adduct containing quasi-molecular ions. The ions formed are guided by electric fields into the mass analyser.

An alternative ionisation technique that is frequently used for larger molecules such as oligo- and polysaccharides, peptides, proteins and DNA is matrix assisted laser desorption ionisation (MALDI) (Karas *et al.*, 1987). In MALDI, the analyte is co-crystallised with UV absorbing matrix molecules. By exposing the crystals, under vacuum, to a pulsed UV-laser, both matrix and

analyte molecules desorb into the gas phase, and a fraction of the desorbed material is ionised by protonation, cation adducts or deprotonation.

## 4.2.2 Mass analysers

### *Quadrupole*

The quadrupole mass analyser is a  $m/z$ -filter where the ions can pass a central region between four parallel rods (Paul & Steinwedel, 1953). RF potentials including a static component are applied to the rods. Although all potentials vary with time the opposing pair of rods have the same potential, while the other two rods have that same potential but with the opposite sign. When an ion enters the space between the rods it will move towards the rods with the attractive potential, and if the potential changes sign before the ion collides with the rod the ion will change its direction. By constantly changing the potential (oscillating the electric field), the ions can travel through the tunnel in a stable trajectory.  $m/z$ -selective stable trajectories between the rods can be obtained by varying the levels of both the static and oscillating part of the potentials while keeping the ratio between the levels constant. For each such setting of the potential, a specific  $m/z$  can pass between the rods to the detector. By scanning through different potentials, ions of different  $m/z$  can pass the filter. Quadrupole filters have low resolution.

### *Ion Trap*

As the name implies, the ion trap (IT) mass analyser traps ions. The trapping is performed by an oscillating electric field similar to that of a quadrupole mass filter and using criteria for stable trajectories to keep ions of different  $m/z$ -values trapped in between a set of electrodes (Paul & Steinwedel, 1960). By manipulating the potentials, ion trajectories can be  $m/z$ -selectively destabilised and hence ions can be consecutively expelled from the trap according to their  $m/z$  and detected to create a mass spectrum. One of the great advantages of the ion trap is the possibility of running tandem MS in multiple steps ( $MS^n$ ). Selected ions (parent ions of a chosen  $m/z$ ) are accumulated in the trap and all other ions are expelled. The parent ions are fragmented (*e.g.* by collisions with gas inside the trap) and the resulting fragment ions are then expelled from the trap and detected. Further, a fragment ion can be selected, accumulated and allowed to fragment and so on.

### *Time of flight*

In time of flight (TOF) mass analysers, the ions are accelerated in an electric field towards a long and typically cylindrical flight tube. The flight tube is a field free region in which the ions travel before they reach the detector. All ions of the same charge are given the same kinetic energy by the accelerating electric field and lighter ions will thus have a higher velocity than heavier ions. The time it takes the ions to travel through the field free region is therefore correlated with the mass to charge ratio ( $m/z$ ) of the ions. One benefit of TOF is that it is very fast, a broad mass range can be analysed in microseconds. In TOF analysers, the length of the flight tube determines the basic limitation for the resolution. If the flight path is increased, the resolution is improved. However, this is not always applicable in practice and a longer tube can result in signal loss due to angular dispersion of the ion beam or scattering of ions after collision with residual gas molecules. The electrostatic mirror (reflectron) (Mamyrin *et al.*, 1973) can double the flight path without making a longer tube. When using a reflectron at the end of the tube, the direction of the ions is reversed and therefore the detector must be placed on the same side of the flight tube as the ion source. The reflectron also contribute to improved resolution by evening out small differences in initial velocity of the ions.

TOF is a suitable analyser to connect with pulsed ionisation techniques such as MALDI, where the laser pulse provides a fixed starting time at which all ions enter the flight tube allowing measurement of the respective flight times to the detector relative to that time. In order to connect a TOF analyser to a continuous ionisation technique such as ESI an approach called orthogonal injection is used. With orthogonal injection, the continuous ion beam from the ESI source enters the flight tube radially and in between a plate and a grid placed at the end of the flight tube. By applying a short high voltage pulse between the plate and the grid ions currently in that space are pushed through the grid axially into the flight tube. The pushing pulse provides a fixed starting time for the measurement of TOF for the ions. With orthogonal injection, ions have minimal initial velocities in the TOF direction, which is a good basis for achieving high mass resolution and good mass accuracy.

### *Hybrid mass analysers*

Using combinations of different types of mass analysers in MS/MS can combine the benefits of the respective analysers. The IT TOF setup allows for accumulation of ions in the ion trap providing better sensitivity followed by simultaneous ejection to the TOF for mass analysis, which reduces the analysis time compared to the classical scanned ion ejection performed in IT. The TOF

also provides a larger mass range, better mass resolution and mass accuracy than the ion trap. The hybrid between quadrupole and TOF (QTOF) has proven successful providing both very high sensitivity and resolution (Glish & Burinsky, 2008).

### 4.2.3 Fragmentation

In carbohydrate chemistry, MS analysis sometimes provide only the  $m/z$  of the molecular ion. To gain further structural information (type of monosaccharides, their connections and possible substituents) fragmentation (*i.e.* breaking of bonds) is required. Domon and Costello introduced a systematic nomenclature for carbohydrate fragment ions (Domon & Costello, 1988) where  $A_i$ ,  $B_i$ , and  $C_i$  denote fragments where the charge is retained on the non-reducing end. Fragments with the charge retained at the reducing end are denoted  $X_j$ ,  $Y_j$ , and  $Z_j$ . Cleavage of the glycosidic bond can often be achieved rather easily producing either  $B_i$ ,  $C_i$ ,  $Y_j$  or  $Z_j$  fragments. The numbers ( $i/j$ ) indicate which glycosidic bond has been cleaved starting counting from the end where the charge is retained (Figure 23). Fragmentation of the sugar ring (cross-ring fragmentations) is useful for determination of substitution positions. The fragments are labelled  $^{k,l}A_i$  or  $^{k,l}X_j$ . The superscript to the left of the letter indicates which bonds are cleaved. Bonds are numbered clock-wise starting from 0 at the bond between the ring oxygen and C1. The number ( $i/j$ ) refers to the number of glycosidic bonds between the reducing/non-reducing end and the cleavage site. If the reducing end is linked by a glycosidic bond to an aglycone this bond is numbered 0. There are a number of different fragmentation techniques, two of them, collision induced dissociation (CID) and electron transfer dissociation (ETD) are introduced below.

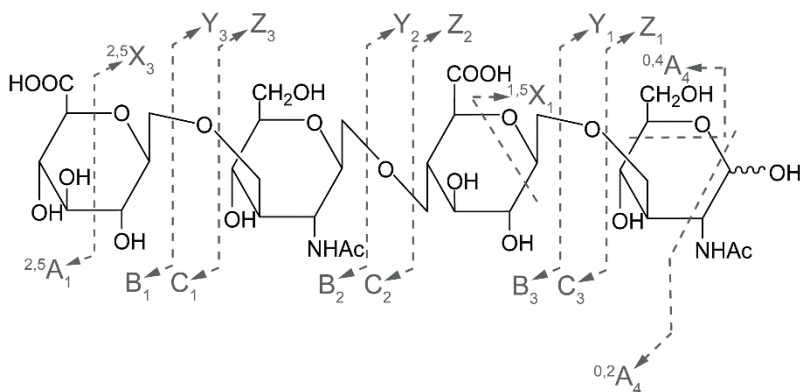


Figure 23. HA tetrasaccharide showing glycosidic cleavages and some possible cross-ring cleavages exemplifying the nomenclature introduced by Domon and Costello (1988). Double cleavage sites are indicated by for example  $Y_1/^{0.2}A_4$ .

### Collision induced dissociation

Deliberate fragmentations resulting from collisional activation are referred to as collision induced dissociation (CID). In collisions between ions and neutral molecules, kinetic energy is transformed to internal energy that can lead to bond breaking in the collided ion and the formation of a fragment ion. The kinetic energy of the ions can be increased by acceleration in order to support fragmentation. Neutral molecules (commonly  $N_2$ , He or Ar) can also be introduced into the mass spectrometer to increase the probability for the occurrence of collisions. CID is compatible with most mass analysers.

### Electron transfer dissociation

For IT mass analysers fragmentation via electron transfer dissociation (ETD) is an alternative to CID. For carbohydrates, the use of ETD has in some studies reported to produce more cross-ring fragmentations as compared to CID.

ETD utilises radical ions created in a CI source. These ions are allowed to react with the parent ions where an electron transfer from the radical ion to the parent ion initiates fragmentation. ETD requires multiply charged parent ions and doping with divalent metal ions have been utilised as a way to increase the charge state (Han & Costello, 2011; Schaller-Duke *et al.*, 2018). Publications using negative mode ETD (NETD) have reported efficient cross-ring fragmentations (Huzarska *et al.*, 2010; Wolff *et al.*, 2010). Unfortunately, NETD is not yet commercially available limiting users to run in positive mode.

## 5 Aims

The properties and applications of hydrogels consisting of hyaluronic acid (HA) cross-linked with 1,4-butanediol diglycidyl ether (BDDE) will depend on their degree of modification, cross-linking and possibly also on the position of substitution of the cross-linker on the polysaccharide. Simple and accurate methods to determine these parameters should be of interest. Understanding the relationships between production parameters, chemical parameters, physical properties and biological effects would facilitate the design of desired hydrogels.

Thus, the general aim of this thesis was to develop methods for, and to investigate the structure of hydrogels consisting of HA cross-linked with BDDE.

Specific aims:

- To develop NMR and MS-based methods for analysis of the position of the linker in HA-BDDE hydrogels.
- To develop a NMR method, that require minimum sample preparation, for quantification of the degree of cross-linking.
- To compare the reactivity of HA and CN towards BDDE.
- To study whether differences in chemical and physicochemical properties of HA-BDDE hydrogels can be related to the degree of cross-linking and manufacturing process.

## 6 Results and discussion

This chapter contains a summary of papers I-IV.

### 6.1 BDPE substitution positions in HA hydrogels – elucidation and method development (Papers I-II)

There are in theory six functional groups on each repeating unit of HA available for modification. Of these six, the four hydroxyls are after deprotonation the strongest nucleophiles and thus most likely to react with the epoxides of BDDE. The relative reactivities of the four hydroxyls are governed by their acidity, steric hindrance and their degree of solvation. The position of substitution might affect physicochemical properties of the hydrogels and could also have biological implications.

#### 6.1.1 Elucidation of substitution positions by NMR

An HA-BDDE hydrogel with MoD of 8% and CrR of 0.1 was used for the study. Since detailed structural analysis of intact hydrogels is difficult due to their high viscosity, the hydrogel was first degraded using the lyase chondroitinase ABC (Kenne *et al.*, 2013). This enzyme cleaves all  $\beta(1\rightarrow4)$  glycosidic linkages down to the disaccharide in unmodified HA, but longer fragments are obtained for HA-BDDE hydrogels. The digest was separated in a two-step procedure using a preparative LC system: i) anionic exchange (Q-sepharose), and ii) size exclusion (Superdex Peptide). Pure fractions containing either di-, tetra- or hexasaccharides of HA with mono-linked BDPE ( $\Delta\text{HA}_2\text{-B}$ ,  $\Delta\text{HA}_4\text{-B}$  and  $\Delta\text{HA}_6\text{-B}$ ) were analysed by NMR.

The  $^1\text{H}$  and  $^{13}\text{C}$  signals were assigned from a combination of 2D NMR spectra and by comparison with NMR data for unsubstituted HA oligosaccharides (Blundell *et al.*, 2006b; Nestor *et al.*, 2010). As expected

upon substitution on sugar rings, upfield shift of  $^1\text{H}$  and downfield shift of  $^{13}\text{C}$  resonances were observed at the position of substitution. The neighboring  $^1\text{H}$  and  $^{13}\text{C}$  NMR signals instead showed opposite chemical shift changes (Figure 24).

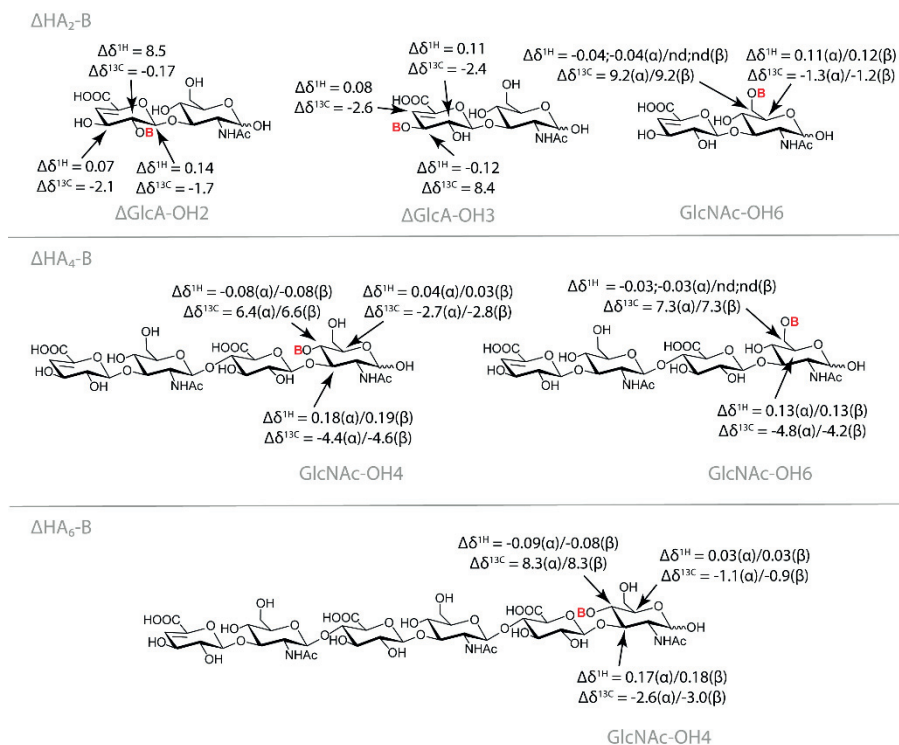


Figure 24. Changes in  $^1\text{H}$  and  $^{13}\text{C}$  chemical shift ( $\Delta\delta$ , ppm) induced by BDPE substitution. **B** = BDPE.

In the  $\Delta\text{HA}_2\text{-B}$  fraction, three different disaccharides were found with substitution by BDPE at position  $\Delta\text{GlcA-OH2}$ ,  $\Delta\text{GlcA-OH3}$ , and  $\text{GlcNAc-OH6}$  respectively (Figure 24). There was no disaccharide with substitution at  $\text{GlcNAc-OH4}$ . Chemical shift reporters allowing quantification of substitution position in the  $^1\text{H}$  NMR spectrum were identified: H1 and H4 of  $\Delta\text{GlcA}$  for substitution at the OH2 and OH3 position respectively (Figure 25a). Integration of these signals gave 52% substitution at  $\Delta\text{GlcA-OH2}$  and 13% at  $\Delta\text{GlcA-OH3}$  leading to 35% substitution at  $\text{GlcNAc-OH6}$ .

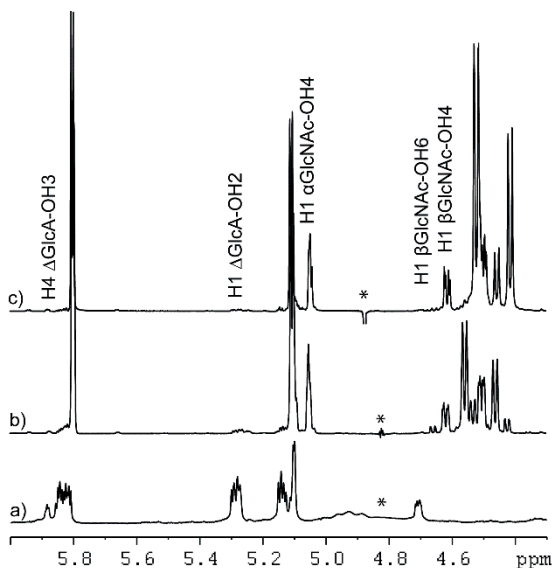


Figure 25. Part of the 1D  $^1\text{H}$  NMR spectra showing the H4 and anomeric proton signals for a)  $\Delta\text{HA}_2\text{-B}$ , b)  $\Delta\text{HA}_4\text{-B}$  and c)  $\Delta\text{HA}_6\text{-B}$ . Chemical shift reporters are indicated. \*Residual HDO signal.

The  $\Delta\text{HA}_4\text{-B}$  fraction revealed the presence of four tetrasaccharides with substitution by BDPE at positions OH2 and OH3 of  $\Delta\text{GlcA}$  and OH4 and OH6 of the reducing end GlcNAc. No BDPE linkage to the internal sugars was observed. Similarly, NMR analysis of  $\Delta\text{HA}_6\text{-B}$  also showed substitutions only on the two terminal residues. Chemical shift reporters of amount of substitution at the different positions were H1 and H4 of  $\Delta\text{GlcA}$  for OH2 and OH3 substitution respectively (as in  $\Delta\text{HA}_2\text{-B}$ ), H1 of GlcNAc ( $\alpha$ ) for OH4 substitution and H1 of GlcNAc ( $\beta$ ) for OH4 and OH6 substitution (Figure 25b, c). In both  $\Delta\text{HA}_4\text{-B}$  and  $\Delta\text{HA}_6\text{-B}$ , OH4 of GlcNAc was the main site of BDPE substitution (72% resp. 92%) followed by GlcNAc-OH6 (21% resp. 6%).

By using dialysis of degraded hydrogel and further SEC/LC-MS separation, cross-linked fragments ( $\Delta\text{HA}_4\text{-B}-\Delta\text{HA}_4$  and  $\Delta\text{HA}_2\text{-B}-\Delta\text{HA}_4$ ) were obtained. Comparison of the 1D  $^1\text{H}$  NMR spectra revealed that the chemical shift reporters identified for mono-linked fragments could be used for cross-linked fragments. Mono- and cross-linked tetrasaccharides displayed almost identical  $^1\text{H}$  spectra and the spectra of  $\Delta\text{HA}_2\text{-B}-\Delta\text{HA}_4$  appeared as the sum of those of  $\Delta\text{HA}_2\text{-B}$  and  $\Delta\text{HA}_4\text{-B}$  (Figure 26).

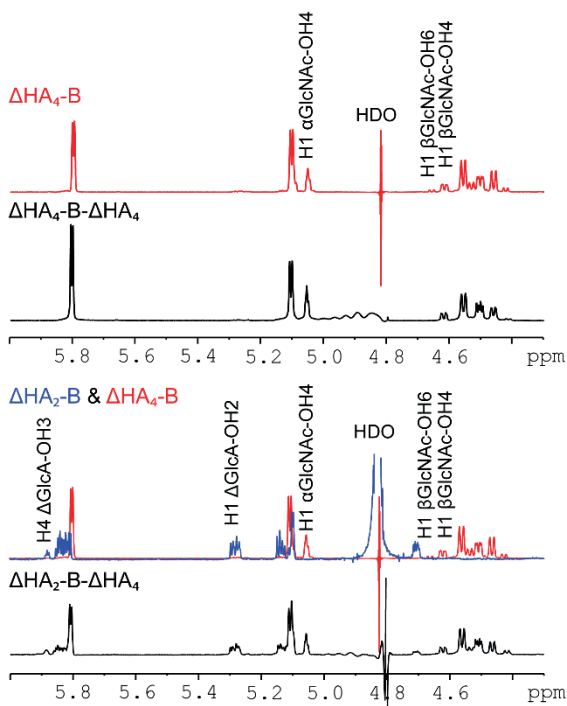


Figure 26. Comparison of part of the 1D  $^1\text{H}$  NMR spectra of  $\Delta\text{HA}_4\text{-B}$  and  $\Delta\text{HA}_4\text{-B-}\Delta\text{HA}_4$  (top) and  $\Delta\text{HA}_2\text{-B}$  overlaid with  $\Delta\text{HA}_4\text{-B}$  and  $\Delta\text{HA}_2\text{-B-}\Delta\text{HA}_4$  (bottom).

$\Delta\text{HA}_6\text{-B}$  could be further degraded into  $\Delta\text{HA}_2$  and  $\Delta\text{HA}_4\text{-B}$  upon addition of more enzyme. Thus, the final products of complete enzymatic degradation of HA-BDDE hydrogels by chondroitinase ABC are  $\Delta\text{HA}_2$ ,  $\Delta\text{HA}_2\text{-B}$ ,  $\Delta\text{HA}_4\text{-B}$ ,  $\Delta\text{HA}_4\text{-B-}\Delta\text{HA}_4$  and  $\Delta\text{HA}_2\text{-B-}\Delta\text{HA}_4$ .

### 6.1.2 Elucidation of substitution positions by MS

In parallel to the structural elucidation by NMR, the fractions  $\Delta\text{HA}_2\text{-B}$  and  $\Delta\text{HA}_4\text{-B}$  were also analysed by LC-MS/MS. The fractions collected as described in 6.1.1 were further separated on a Hypercarb column. The Hypercarb column is a porous graphite column that offers separation based on the area of the analyte that is in contact with the stationary phase and on charge-induced dipoles. This allows for separation of geometric and positional isomers. For  $\Delta\text{HA}_2\text{-B}$ , a total of twelve different isomers (ten resolved chromatographic peaks) were detected, representing six pairs of  $\alpha$  and  $\beta$  anomers (Figure 27). For substitution at all four hydroxyl groups, a maximum of eight peaks, two anomers for each position of substitution, would be expected. See section 6.1.3 for clarification.

Fragmentation of the glycosidic bond provided information about which of the two monosaccharides that was substituted. Extracted ion chromatograms (negative mode) of glycosidic bond cleavage ion  $C_1$  revealed eight isomers with substitution at  $\Delta\text{GlcA}$  ( $C_1 = m/z\ 395$ ) and four isomers with substitution at  $\text{GlcNAc}$  ( $C_1 = m/z\ 175$ ) (Figure 27). MS/MS of the sodiated parent ion in positive mode ( $m/z\ 622$ ) revealed three groups (A, B, C) of UV chromatographic peaks with identical mass spectra, A: peaks 1, 2, 5 and 7, B: peaks 9 and 10, and C: peaks 3, 4, 6 and 8. Analysis of cross-ring fragments in the MS/MS spectra demonstrated substitution at position  $\Delta\text{GlcA-OH}_2$  for group A,  $\Delta\text{GlcA-OH}_3$  for group B and  $\text{GlcNAc-OH}_6$  for group C (Figure 27). Integration of peaks in the UV chromatogram showed that the relative amount of substitution was 55%, 13% and 24% for  $\Delta\text{GlcA-OH}_2$ ,  $\Delta\text{GlcA-OH}_3$  and  $\text{GlcNAc-OH}_6$  respectively. These results were in very good agreement with the NMR data.

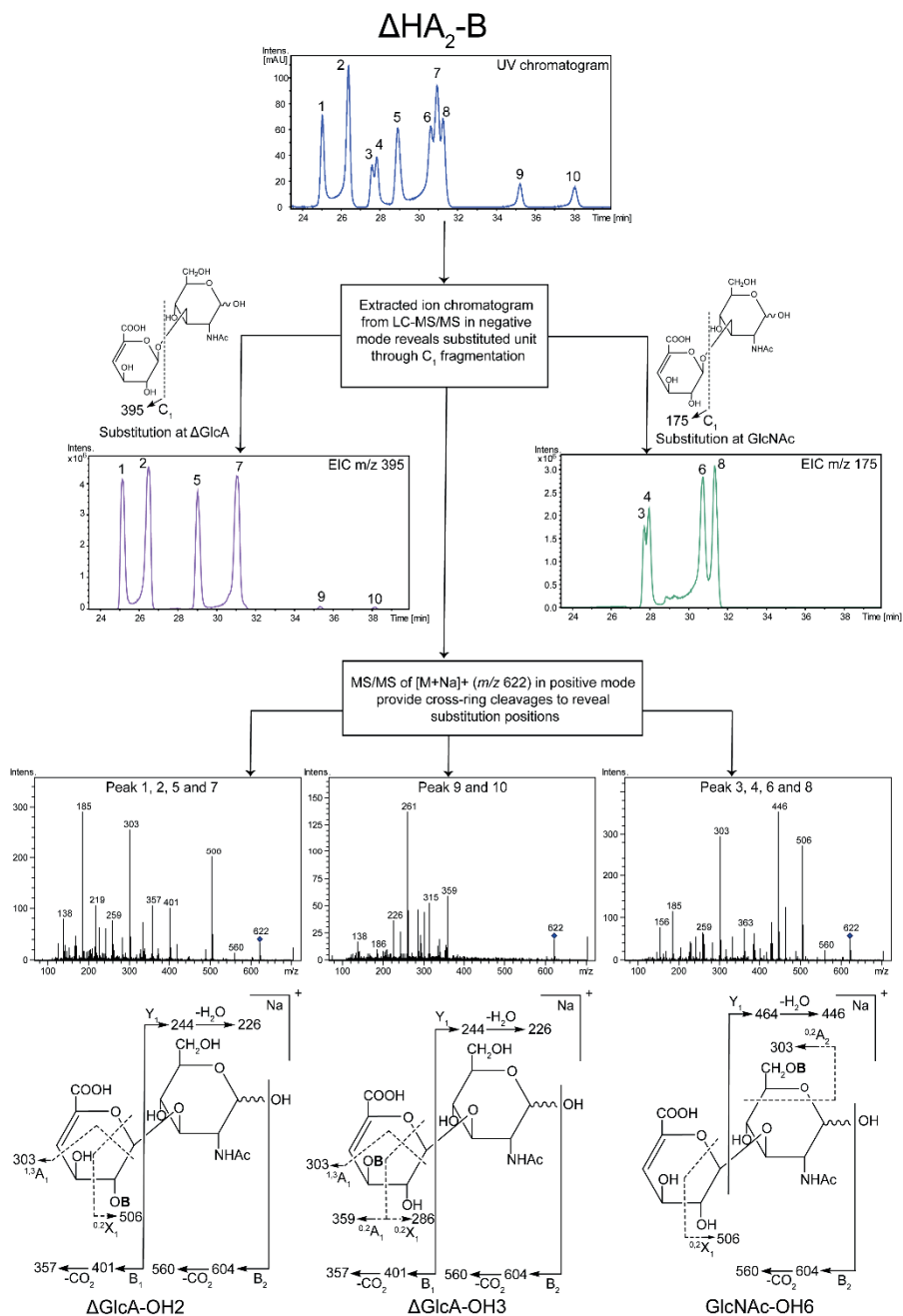


*Figure 27.* Representation of the liquid chromatography separation coupled with MS analysis used to reveal the positions of substitution by BDPE in the  $\Delta\text{HA}_2\text{-B}$  fragment. Peaks belonging to  $\alpha$  anomers of disaccharides substituted at  $\Delta\text{GlcA-OH3}$  are overlapping with peaks 5 and 8.

### 6.1.3 Configuration of BDPE

As seen earlier, each substitution position by BDPE in  $\Delta$ HA<sub>2</sub>-B gave rise to four chromatographic peaks instead of the two expected. Moreover, additional splitting of some signals was observed in the NMR spectra of the different fragments (see Paper I). These peaks were attributed to the *R/S* chirality of BDPE, giving the four isomers depicted in Figure 28.

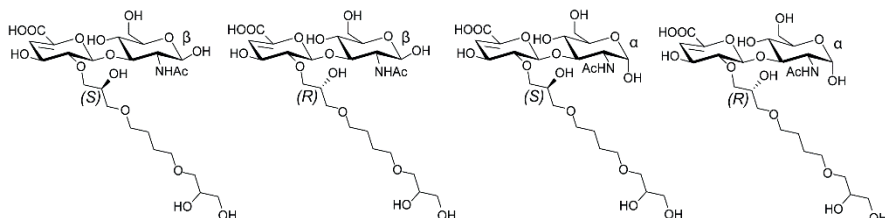


Figure 28. Schematic of the four isomers observed for  $\Delta$ HA<sub>2</sub>-B with substitution by BDPE at GlcA-OH<sub>2</sub>. GlcNAc can be either the  $\alpha$  or  $\beta$  configuration and BDPE can have either the *R* or *S* configuration. BDPE has two chiral centres but only the one closest to HA affected the analysis.

This was confirmed by synthesising a hydrogel using enantiomerically enriched BDDE. Hydrolytic kinetic resolution was used to separate (2'*R*,2''*R*)-BDDE from racemic BDDE. The enantiomeric excess was confirmed using a chiral HPLC column. The new hydrogel was prepared using the same experimental conditions as for racemic BDDE. Enzymatic degradation of the new hydrogel and chromatographic separation provided oligosaccharides with (2'*R*,2''*R*)-BDDE. Subsequent NMR and LC-MS analysis confirmed that the additional signals originated from a diastereomeric mixture (see Paper I).

### 6.1.4 Development of 1D <sup>1</sup>H NMR method for quantification of substitution positions in HA hydrogels

In Papers I and II, analysis of HA-BDDE fragments of different sizes led to the identification of chemical shift reporters for each of the four substitution positions of BDPE allowing quantification from 1D proton NMR spectra. These chemical shift reporters were valid for all differently sized fragments, both mono- and cross-linked for a given substitution position (*i.e.* independent of the type of fragment). In Paper II, we thus developed a 1D <sup>1</sup>H NMR method for analysis of the distribution of substitution position in HA-BDDE hydrogels.

The protocol included four steps: i) washing of the gels to remove free HA and BDDE, ii) incubation with chondroitinase ABC, iii) lyophilisation (optional), iv) 1D <sup>1</sup>H NMR analysis. No chromatographic separation is required. Six samples with varying MoD and CrD were analysed. A relaxation delay of 30 s was used to obtain quantitative NMR spectra. A typical <sup>1</sup>H NMR spectrum

is shown in Figure 29 together with the four signals used for quantification of the relative amount of substitution at each of the four hydroxyls. The only signal suffering from some overlap is the GlcNAc-H1 $\alpha$  signal representing substitution at GlcNAc-OH6. It overlaps with the corresponding signal of the unsubstituted disaccharide, which is the major component of the hydrogel digest (in general > 90%). Figure 30 shows the same trend for all six hydrogels, namely that GlcNAc-OH4 is the most common substitution position followed by  $\Delta$ GlcA-OH2 and GlcNAc-OH6. The amount of substitution at  $\Delta$ GlcA-OH3 was very small.

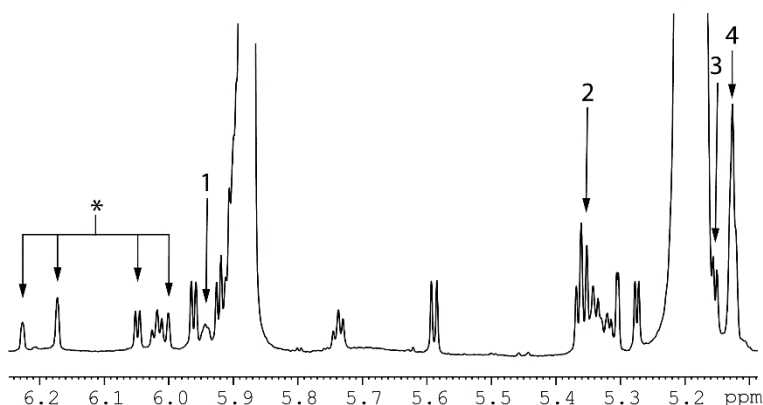


Figure 29. Anomeric region of a 1D  $^1\text{H}$  NMR spectrum of a HA-BDDE hydrogel after enzymatic degradation indicating 1)  $\Delta$ GlcA-H4 of  $\Delta\text{HA}_x$  substituted at  $\Delta$ GlcA-OH3, 2)  $\Delta$ GlcA-H1 of  $\Delta\text{HA}_x$  substituted at  $\Delta$ GlcA-OH2, 3) GlcNAc-H1 $\alpha$  of  $\Delta\text{HA}_x$  substituted at  $\alpha$ -GlcNAc-OH6, 4) GlcNAc-H1 $\alpha$  of  $\Delta\text{HA}_x$  substituted at  $\alpha$ -GlcNAc-OH4. The asterisk (\*) highlights signals H1 and H3 from  $\alpha/\beta$ -(*E*)-3-dehydroxy-2-en-D-GlcNAc (peeling product). The two largest signals correspond to H1 and H4 of  $\Delta\text{HA}_2$ .

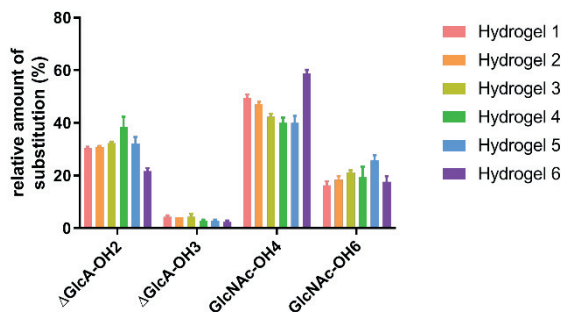


Figure 30. Relative percentage of BDPE substitution at the four hydroxyls of the HA repeating unit in six different HA-BDDE hydrogels.

A number of additional signals visible in the 1D  $^1\text{H}$  NMR spectra were mainly due to peeling from the reducing end GlcNAc resulting in formation of (*E*)-3-dehydroxy-en-D-GlcNAc and leaving a GlcA reducing end. As can be seen in Figure 29, these signals do not interfere with the signals of interest. The peeling product (*E*)-3-dehydroxy-en-D-GlcNAc is commonly found in degraded HA, but the factors that trigger the peeling are not clearly understood. The structure of the peeling product has been reported previously (Blundell *et al.*, 2006b) but not the full assignment of the NMR signals (Paper II, SI).

## 6.2 1D $^{13}\text{C}$ NMR method for determination of degree of cross-linking (Paper II)

The effective cross-linker ratio (CrR) in HA-BDDE hydrogels can be determined by LC-MS (Kenne *et al.*, 2013), but the method is time consuming and labour intensive. An alternative method would therefore be of interest. Using the same sample preparation as for the determination of substitution positions by  $^1\text{H}$  NMR, a protocol for determination of the degree of cross-linking (CrD) from 1D  $^{13}\text{C}$  NMR spectra was developed.

The requirement was to sort out and identify distinctive signals representative of mono- or cross-linked fragments that could be integrated to obtain CrR. Comparison of the  $^1\text{H}$ - $^{13}\text{C}$  HSQC spectra of mono- and cross-linked fragments revealed two distinctive cross-peaks corresponding to the H10'/C10' ( $\delta$  3.58-3.66/62.7 ppm). They belong to the primary alcohol of mono-linked BDPE and were thus not present in the cross-linked fragments (Figure 31). HSQC is a very sensitive NMR experiment but integration of cross peaks is not yet straightforward. 1D  $^1\text{H}$  NMR spectra could not be used either because of overlap of signals but the C10' signal at  $\delta$  62.7 ppm was well resolved from other signals in the 1D  $^{13}\text{C}$  NMR spectra.

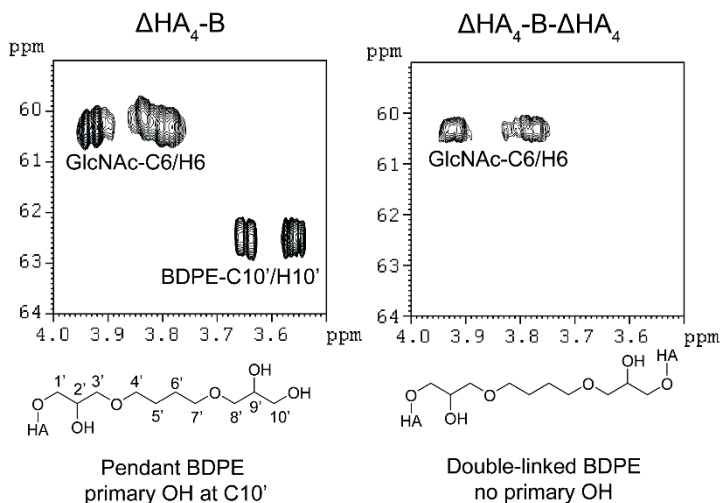


Figure 31. Portion of the  $^1\text{H}$ - $^{13}\text{C}$  HSQC NMR spectra of (left) mono-linked and (right) cross-linked HA-BDDE tetrasaccharides.

The signal at  $\delta$  62.7 ppm represents the amount of mono-linked BDPE. The C5' and C6' of BDPE have the same  $^{13}\text{C}$  chemical shift at  $\delta$  25.2 ppm in both mono- and double-linked BDPE and can thus represent the total amount of BDPE. Integration of these signals (Figure 32) allows for calculation of CrR according to Equation 5.

$$\text{CrR} = 1 - I^{\delta\text{C}62.7} / (I^{\delta\text{C}25.2} / 2) \quad (\text{Eq. 5})$$

The degree of modification can also be determined from the same 1D  $^{13}\text{C}$  NMR spectra. The signals at  $\delta$  21.9-22.6 ppm belonging to the acetamido group represent the total number of HA disaccharides (Figure 32). These signals together with the signal at  $\delta$  25.2 ppm allow for calculation of MoD according to Equation 6.

$$\text{MoD} = (I^{\delta\text{C}25.2} / 2) / I^{\delta\text{C}(21.9-22.6)} \quad (\text{Eq. 6})$$

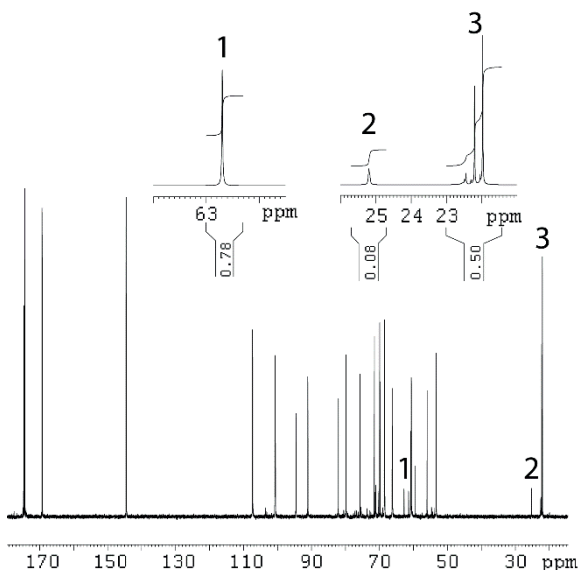


Figure 32.  $^{13}\text{C}$  NMR spectrum of a HA-BDDE hydrogel after enzymatic degradation by chABC. The signals used for calculation of MoD and CrR are indicated: 1) C10' of mono-linked BDPE, 2) C5' and C6' of mono- and double-linked BDPE, and 3) methyl carbon from the acetamido group of GlcNAc.

The 1D  $^{13}\text{C}$  NMR spectra were collected with an inverse gated decoupling experiment using a relaxation delay of 15 s. Deconvolution of spectra was performed prior to integration. The MoD and CrD (CrR x MoD) values obtained from integration of the signals indicated in Figure 32 are presented in Figure 33. The MoD values obtained by  $^{13}\text{C}$  NMR were in good agreement with those obtained by  $^1\text{H}$  NMR, thus confirming that 1D  $^{13}\text{C}$  NMR could be used for analysis of CrR. The CrD values obtained from the  $^{13}\text{C}$  NMR spectra were similar to those obtained from the SEC/LC-MS method (Kenne *et al.*, 2013). The method however has some limitations for HA-BDDE hydrogels with MoD < 1% due to the very low intensities of the BDPE signals.

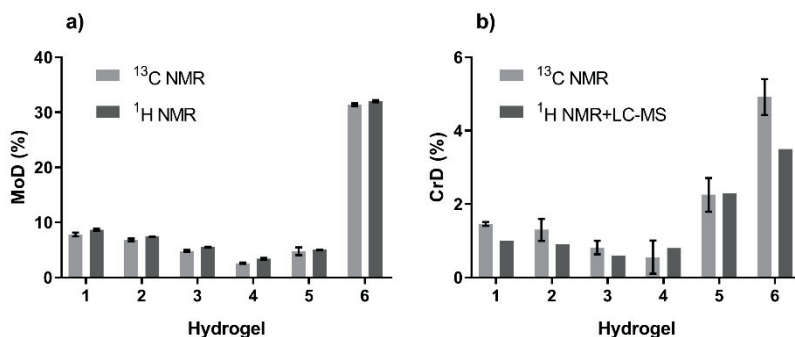


Figure 33. a) MoD and b) CrD obtained for the six hydrogels. The NMR analysis were made in triplicates and the error bars indicate the standard deviation.

### 6.3 Comparison of reactivity of HA and CN toward BDDE and alkali induced changes (Paper III)

To investigate the effect of configuration at C4 of the aminoglycan, the position of substitutions of BDPE on CN were determined. The alkali-induced changes in <sup>1</sup>H and <sup>13</sup>C chemical shifts were determined for HA, HA<sub>4</sub> and CN. The <sup>1</sup>H chemical shifts and temperature coefficients of the exchangeable protons of HA and CN polysaccharides were measured.

#### 6.3.1 Substitution positions of BDPE on CN

A hydrogel was obtained by cross-linking CN with BDDE using the same experimental conditions as for HA-BDDE hydrogels. The substitution positions of BDPE were identified using the same methodology as for HA in Paper I. The separation profiles of HA-BDDE and CN-BDDE fragments on a size exclusion LC column are displayed in Figure 34. The degradation of the CN-BDDE hydrogel was more extensive than that of the HA-BDDE hydrogel where larger fragments remain. In Paper I, it was shown that HA-BDDE cannot be degraded down to disaccharide units when substitution by BDPE occurred at position 4 of GlcNAc. Since this position is the most common substitution position in HA-BDDE hydrogels, the ΔHA<sub>2</sub>-B fragment was not very abundant (see Paper I). Upon enzymatic degradation of CN-BDDE hydrogels, the corresponding fragment (ΔCN<sub>2</sub>-B) was the most abundant BDPE-linked fragment (Figure 34).

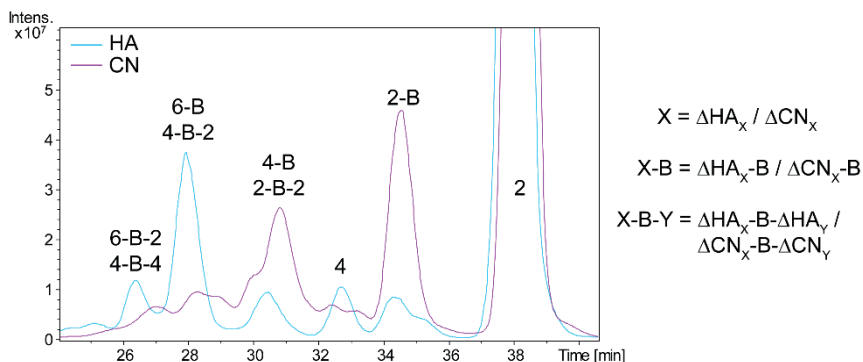
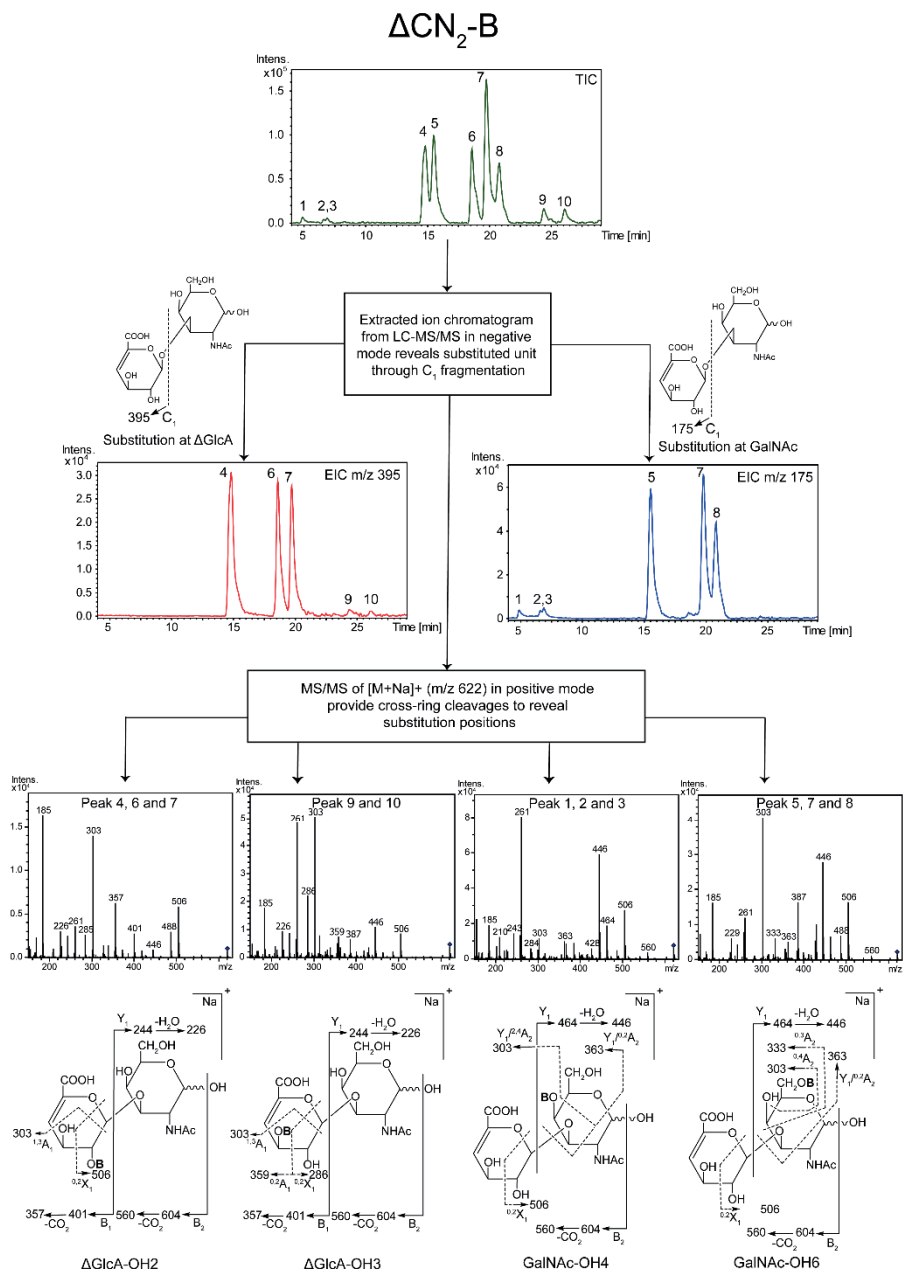


Figure 34. Separation profile (TIC) for HA-BDDE and CN-BDDE degraded with chondroitinase ABC.  $\Delta\text{HA}_6\text{-B}$  is the most abundant BDPE-linked fragment in the HA-BDDE digest but it can be further degraded to  $\Delta\text{HA}_2$  and  $\Delta\text{HA}_4\text{-B}$ .

NMR analysis of the fragments showed that the amount of substitution at  $\Delta\text{GlcA-OH}_2$  was much higher than at  $\Delta\text{GlcA-OH}_3$ . Elucidation of substitution positions on GalNAc was more complicated due to i) small amount of compound with substitution at GalNAc-OH4, and ii) no transfer of magnetization from C4/H4 to C5/H5 in the TOCSY and HSQC-TOCSY spectra due to small  $^3J_{\text{H}_4,\text{H}_5}$  coupling constant (Sattelle *et al.*, 2010) hindering unambiguous determination of C5/H5 and C6/H6 signals.

LC-MS analysis of the  $\Delta\text{CN}_2\text{-B}$  fraction using the same methodology as for  $\Delta\text{HA}_2\text{-B}$  in Paper I demonstrated the presence of four disaccharides, each with different position of substitution for BDPE (Figure 35). The total ion chromatogram revealed that peaks corresponding to the disaccharides with substitution at  $\Delta\text{GlcA-OH}_2$  and GalNAc-OH6 displayed similar intensities and appeared much more intense than peaks corresponding to the disaccharides with substitution at  $\Delta\text{GlcA-OH}_3$  and GalNAc-OH4. As for  $\Delta\text{HA}_2\text{-B}$ , there were four chromatographic peaks for each position of substitution. By collection and reinjection of fractions, all the matching anomeric pairs were identified (Figure 36). Since substitution by BDPE can occur at all four hydroxyl groups in the  $\Delta\text{CN}_2\text{-B}$  fraction, it could be concluded that an axial substituent on the aminosugar does not prevent the enzyme from cleaving the  $\beta(1\rightarrow4)$  glycosidic bond.



**Figure 35.** Representation of the liquid chromatography separation coupled with MS analysis used to reveal the positions of substitution by BDPE in the  $\Delta\text{CN}_2\text{-B}$  fragment.

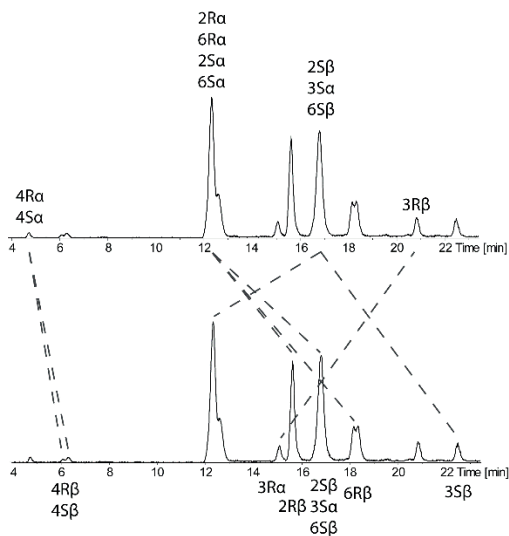


Figure 36. Schematic representation of the determination of anomeric pairs among the sixteen isomers of  $\Delta\text{CN}_2\text{-B}$ . The peaks indicated in the top TIC gave the corresponding peaks in the bottom TIC upon mutarotation. Separation was performed on a Hypercarb column.

### 6.3.2 Alkali induced changes in $^1\text{H}$ and $^{13}\text{C}$ chemical shifts

Alkali titration monitored by NMR gives site-specific information about the deprotonation. Both  $^1\text{H}$  and  $^{13}\text{C}$  NMR have been utilised for this purpose in *e.g.* heparin (Wang *et al.*, 1991), sucrose (Popov *et al.*, 2006), mannitol (Gaidamauskas *et al.*, 2005) and cyclodextrin (Gaidamauskas *et al.*, 2009). Deprotonation causes increased electronegativity of the carbons attached to the deprotonation site resulting in downfield shifts (Gaidamauskas *et al.*, 2009). In sugars, all carbons are normally shifted downfield with increased change in chemical shift for higher proximity to the deprotonation site (Popov *et al.*, 2006).

HA, CN polysaccharides (85 resp. 33 kDa) and HA tetrasaccharide were analysed by NMR spectroscopy in the pH range 7-14. In HA, the largest downfield shift change ( $\Delta\delta^{13\text{C}(\text{pH})}$ ) for a hydroxyl bearing carbon was observed for C4 of GlcNAc followed by C6 of GlcNAc. C3 of GlcA was very little affected by alkali while C2 of GlcA experienced a large upfield shift. Since C1 of GlcA and C3 of GlcNAc were also upfield shifted, these unusual changes were attributed to loss of the GlcA(O5)-GlcNAc(OH4) hydrogen bond resulting in a change in conformation. These data also previously reported by Bociek *et al.* in 1980 have, to our knowledge, not been further discussed (Bociek *et al.*, 1980). The HA tetrasaccharide showed the same pattern as the HA polysaccharide (Figure 37) suggesting that the effect was a result of local conformational change and not disruption of intermolecular interactions.

In the CN polysaccharide, the alkali induced changes in chemical shifts were small in comparison with HA. This could be due to higher  $pK_a$  of the hydroxyls in CN. All four hydroxyl bearing carbons were downfield shifted. However, slight upfield shift were measured for C1 of GlcA and C2 and C3 of GalNAc.

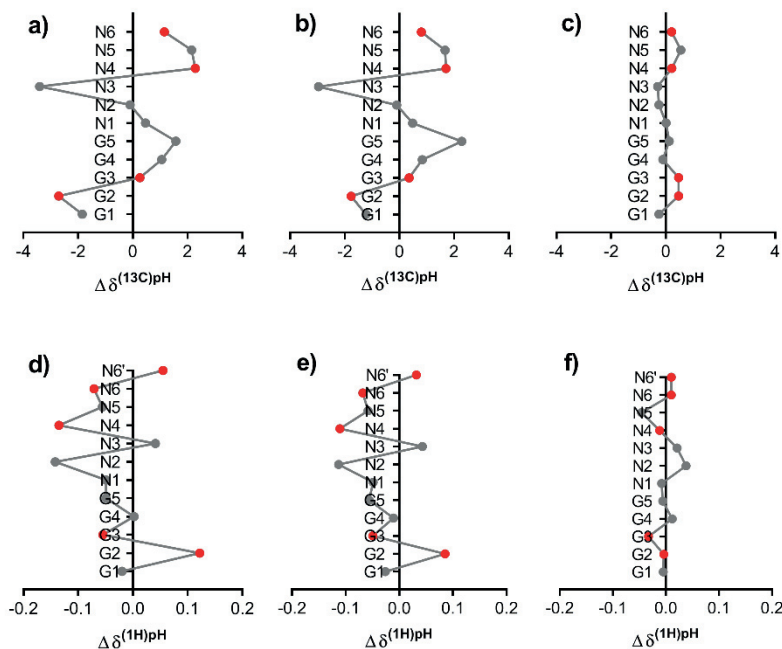


Figure 37. Alkali induced changes in chemical shifts ( $\Delta\delta^{pH} = \delta^{\text{high pH}} - \delta^{\text{low pH}}$ ) for HA polysaccharide (a and d), HA tetrasaccharide (b and e) and CN polysaccharide (c and f). Hydroxyl bearing carbons are marked in red.

### 6.3.3 NMR of exchangeable protons

The temperature coefficients ( $d\delta/dT$ ) of the hydroxyl protons and the changes in their chemical shifts compared to those in the corresponding methyl glucosides ( $\Delta\delta^{\text{OH}}$ ) were determined for both HA and CN. This allowed for comparison of hydrogen bonding and hydration in the two polysaccharides. The data indicated that GlcA-OH3 and GlcNAc-OH4 of HA are involved in transient hydrogen bonding with the neighbouring ring oxygen ( $d\delta/dT = -9.3$  and  $-8.1$  ppb/ $^{\circ}\text{C}$ ,  $\Delta\delta^{\text{OH}} = -0.5$  and  $-0.8$  ppm) which is in agreement with previous studies (Blundell *et al.*, 2006a; Nestor *et al.*, 2010; Nestor & Sandström, 2017). In contrast, GalNAc-OH4 of CN had a  $d\delta/dT$  of  $-12.5$  ppb/ $^{\circ}\text{C}$  and  $\Delta\delta^{\text{OH}}$  of  $0.07$  revealing that the axial orientation of OH4 does not allow for hydrogen bonding to

GlcA-O5. The relatively large negative  $\Delta\delta^{\text{OH}}$  of GlcA-OH2 and GlcA-OH3 indicated the presence of transient hydrogen bonding to the acetamido group and the neighbouring ring oxygen (GlcNAc-O5) respectively (Figure 38). These results show the simple use of  $\Delta\delta^{\text{OH}}$  for indicating the occurrence of hydrogen bonding in two related compounds.

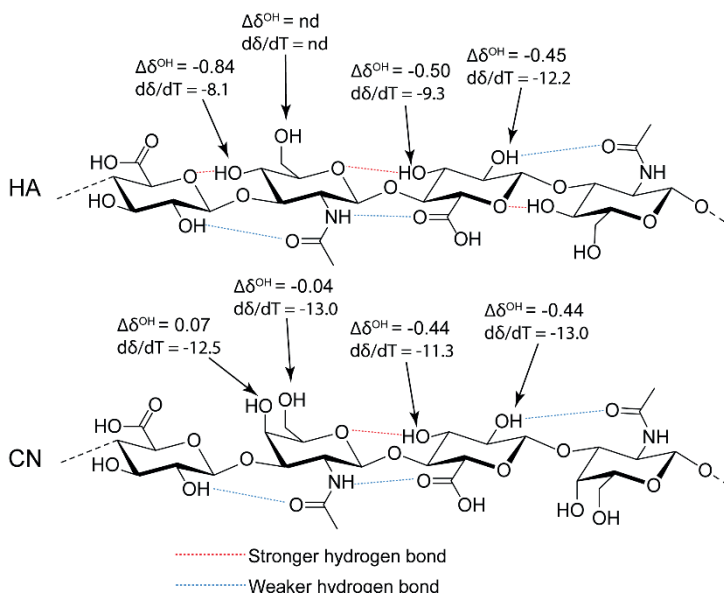


Figure 38. Temperature coefficient ( $d\delta/dT$ , ppb/°C) and change in chemical shift compared to the corresponding hydroxyl proton in the methyl glycoside ( $\Delta\delta^{\text{OH}}$ , ppm).

## 6.4 Relaxation and diffusion of water protons in HA solutions and hydrogels – comparison with physicochemical parameters (Paper IV)

The differences in chemical properties of hydrogels (degree of modification, degree of cross-linking, substitution positions and substitution pattern) affect the physical properties of the hydrogels (viscoelastic behaviour, swelling degree, gel content). In this study we measured the longitudinal ( $T_1$ ) and transverse ( $T_2$ ) relaxation times and diffusion coefficients ( $D$ ) of water protons in nine hydrogels (A-I) with varying properties (Table 2) using high-field NMR spectroscopy. The hydrogels were analysed at different HA concentrations (2.5, 5 and 10 mg/ml) and temperatures (5-50 °C). For comparison, native HA of three different molecular weights (85, 172 and 3000 kDa) were also studied.

Table 2. Chemical and physicochemical parameters for hydrogels (A-I)

Hydrogel	Intrinsic viscosity* (m <sup>3</sup> /kg)	MoD (%)	CrR	CrD (%)	GelC (%)	SwD (g/g)	G' (Pa)	G'' (Pa)	tan $\delta$
A	2.8	7.4	0.1	0.8	93.9	173	870	75	0.09
B	1.7	1.0	0.2	0.2	88.7	144	741	101	0.14
C	1.8	1.1	0.5	0.5	88.0	226	401	27	0.07
D	1.8	1.5	0.5	0.8	96.3	116	1845	188	0.10
E	1.8	1.1	0.3	0.3	77.8	887	45	14	0.32
F	2.9	7.0	0.1	1.0	76.3	827	66	18	0.28
G	1.9	0.9	0.3	0.2	62.9	542	109	23	0.21
H	0.26	4.6	0.5	2.1	98.0	79	2053	304	0.15
I	2.8	2.9	0.2	0.6	86.7	359	288	15	0.05

\*of HA raw material before cross-linking

#### 6.4.1 Longitudinal relaxation ( $T_1$ ) and diffusion coefficient ( $D$ ) of water protons

A small dependence of the  $T_1$  and  $D$  of water protons with concentration of HA could be attributed to the degree of water molecules bound to the polymer. However, the same behaviour was observed for all samples and it is only at the highest temperatures that  $T_1$  and  $D$  of the water protons in the HA samples were slightly different from a water reference sample (Figure 39).

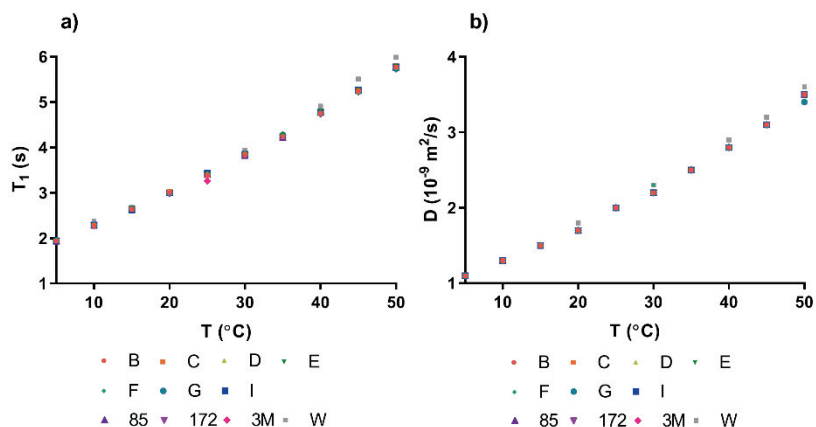


Figure 39. a)  $T_1$  and b)  $D$  for water protons as a function of temperature in HA hydrogels **B-G, I**, three HA solutions (5 mg/ml) and the water reference sample (W). Solvent 9:1 H<sub>2</sub>O:D<sub>2</sub>O.

#### 6.4.2 Transverse relaxation ( $T_2$ ) of water protons

At high-field NMR,  $T_2$  relaxation is mainly dominated by chemical exchange between water protons and polysaccharide hydroxyl protons (Hills *et al.*, 1989). There is a clear correlation between the  $T_2$  of water protons and concentration of HA (Figure 40a). At the lowest concentration (2.5 mg/ml), there is a continuous increase in  $T_2$  within the measured temperature range. The strongest hydrogel (**D**) shows the lowest  $T_2$  while the 85 kDa HA solution shows the highest  $T_2$ . The  $T_2$  in hydrogels **B**, **C**, **E** and **F** show a behaviour similar to the  $T_2$  in the 3 MDa HA solution (Figure 40a). For the 5 mg/ml concentration, the HA solutions show a maximum  $T_2$  around 25-35 °C. Hydrogels **C** and **D** also show a maximum  $T_2$  while for the others, the  $T_2$  curves flatten out or show a slight increase at high temperatures (Figure 40b). For the highest concentration (10 mg/ml), all samples show maxima at low temperatures (10-20 °C). The strongest hydrogel **H** shows the lowest  $T_2$ . The maxima of the 85 and 172 kDa samples are followed by a steep decrease in  $T_2$  with increasing temperature (Figure 40c).

The dependence of  $T_2$  of the water protons with concentration and molecular weight of HA can be associated with a lower mobility of water at higher concentration/molecular weight resulting in shorter  $T_2$ . The varying temperature profiles of  $T_2$  indicates contribution from both  $T_2$  of the water protons (longer) and  $T_2$  of the exchangeable protons of HA (very short). At low temperatures, the chemical exchange is slow and thus its contribution to  $T_2$  is small.  $T_2$  of water protons increase with temperature and this is what we observe at low temperatures. As temperature increase, so does the chemical exchange and  $T_2$  of the exchangeable protons from the polymer contribute more to the measured  $T_2$ .

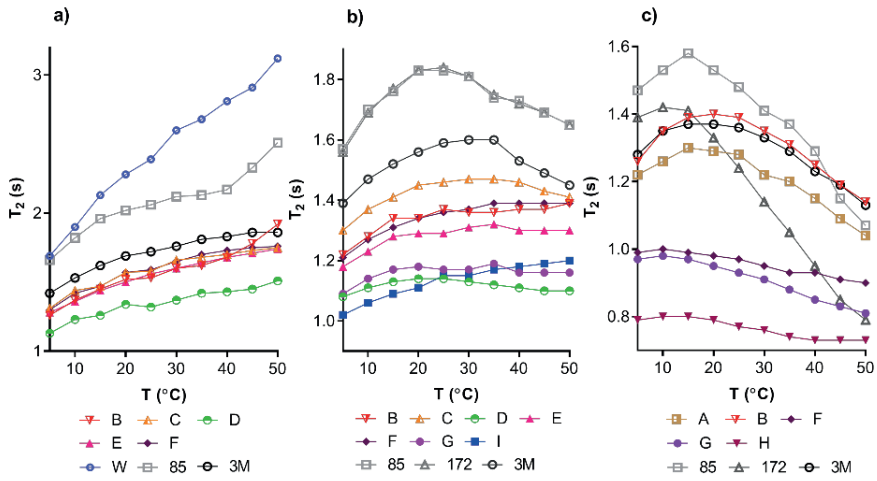


Figure 40.  $T_2$  of water protons as a function of temperature ( $^{\circ}\text{C}$ ) in HA hydrogels and solutions at three different HA concentrations: a) 2.5, b) 5 and c) 10 mg/ml. W = water reference sample ( $\text{H}_2\text{O}/\text{D}_2\text{O}$  9:1).

## 7 Conclusion and future perspectives

The major purpose of this project has been to study the structure and properties of HA hydrogels cross-linked by BDDE.

- Extensive MS and NMR studies performed on isolated HA-BDDE fragments, obtained from degradation of the hydrogel by chondroitinase, have led to the identification of the position of substitution of the cross-linker.
- Substitution by BDPE occurred at all four hydroxyls on the HA repeating unit. GlcNAc-OH4 was the most common substitution position, followed by GlcA-OH2 and GlcNAc-OH6. Substitution at GlcNAc-OH4 was found to hinder chondroitinase from cleaving the tetrasaccharide down to disaccharide units.
- Identification of chemical shift reporters has led to the development of simple and reliable 1D  $^1\text{H}$  and  $^{13}\text{C}$  NMR methods for i) quantification of the relative amount of substitution at each position on HA and ii) determination of the degree of cross-linking without any requirement for chromatographic separation.
- CN differs from HA only by the configuration at C4 of the amino sugar. In CN-BDDE hydrogels, substitution on CN occurred at all four hydroxyls. GalNAc-OH6 and GlcA-OH2 were the major sites of substitution. Common for both HA and CN was a low amount of substitution at GlcA-OH3. Substitution at GalNAc-OH4 on CN did not hinder enzymatic degradation by chondroitinase down to disaccharides.
- The alkali-induced changes in chemical shift suggested that HA has a lower  $\text{pK}_a$  than CN and that high pH results in a change in conformation of HA at the  $\beta(1\rightarrow3)$  glycosidic linkage. The largest downfield shift of a hydroxyl bearing carbon was observed for C4 of GlcNAc, indicating that it is the first hydroxyl to be deprotonated on HA.

- Transient hydrogen bonding was observed in both HA and CN between GlcA-OH3 and O5 of the aminoglycan, as well as between GlcA-OH2 and the carbonyl of the acetamido group. However, hydrogen bonding between OH4 of the aminoglycan and GlcA-O5 was only present in HA.
- Transverse relaxation of water protons in HA-BDDE hydrogels or HA solutions is mainly governed by chemical exchange between water protons and HA hydroxyl protons and its study as a function of temperature gives information on the mobility of the polysaccharide. Preliminary data show no clear correlation between the physicochemical properties of the hydrogels and the water relaxation. However, some correlation between mobility and gel strength is observed.

The following studies would be of interest to further improve the knowledge on HA-BDDE hydrogels:

- ❖ Analysis of the degree of cross-linking by NMR would be easier if cross-peaks in  $^1\text{H}$ - $^{13}\text{C}$  HSQC NMR spectra could be quantified in a reliable way.
- ❖ Analysis of the cross-link distribution on the HA chain and its influence on the properties of the hydrogel.
- ❖ Investigate if and how the positions of substitution of the cross-linker on HA influence the physicochemical properties of the hydrogel.
- ❖ Investigate if and how the positions of substitution of the cross-linker on HA has biological implications, such as influence on the rate of degradation of the hydrogels by hyaluronidases.
- ❖ Investigate if hydrogels with regiospecific position of substitution of the cross-linker on HA can be synthesised.

## References

- Al-Sibani, M., Al-Harrasi, A. & Neubert, R. H. H. (2017) 'Effect of hyaluronic acid initial concentration on cross-linking efficiency of hyaluronic acid - based hydrogels used in biomedical and cosmetic applications', *Pharmazie*, 72(2), 81-86.
- Almond, A. (2005) 'Towards understanding the interaction between oligosaccharides and water molecules', *Carbohydrate Research*, 340(5), 907-920.
- Almond, A., DeAngelis, P. L. & Blundell, C. D. (2006) 'Hyaluronan: The local solution conformation determined by NMR and computer modeling is close to a contracted left-handed 4-fold helix', *Journal of Molecular Biology*, 358(5), 1256-1269.
- Atmuri, V., Martin, D. C., Hemming, R., Gutsol, A., Byers, S., Sahebjam, S., Thliveris, J. A., Mort, J. S., Carmona, E., Anderson, J. E., Dakshinamurti, S. & Triggs-Raine, B. (2008) 'Hyaluronidase 3 (HYAL3) knockout mice do not display evidence of hyaluronan accumulation', *Matrix Biology*, 27(8), 653-660.
- Balazs, E. A., Laurent, T. C. & Jeanloz, R. W. (1986) 'Nomenclature of hyaluronic acid', *Biochemical Journal*, 235(3), 903.
- Balazs, E. A. & Leshchiner, A. (1986) *Cross-linked gels of hyaluronic acid and products containing such gels*. United States 4582865
- Barbucci, R., Consumi, M., Lamponi, S. & Leone, G. (2003) 'Polysaccharides based hydrogels for biological applications', *Macromolecular Symposia*, 204(1), 37-58.
- Barbucci, R., Leone, G., Chiumiento, A., Di Cocco, M. E., D'Orazio, G., Gianferri, R. & Delfini, M. (2006) 'Low- and high-resolution nuclear magnetic resonance (NMR) characterisation of hyaluronan-based native and sulfated hydrogels', *Carbohydrate Research*, 341(11), 1848-1858.
- Barbucci, R., Rappuoli, R., Borzacchiello, A. & Ambrosio, L. (2000) 'Synthesis, chemical and rheological characterization of new hyaluronic acid-based hydrogels', *Journal of Biomaterials Science-Polymer Edition*, 11(4), 383-399.
- Bekiroglu, S., Sandström, A., Kenne, L. & Sandström, C. (2004) 'Ab initio and NMR studies on the effect of hydration on the chemical shift of hydroxy protons in carbohydrates using disaccharides and water/methanol/ethers as model systems', *Organic & Biomolecular Chemistry*, 2(2), 200-205.
- Bleakney, W. (1929) 'A new method of positive ray analysis and its application to the measurement of ionization potentials in mercury vapor', *Physical Review*, 34(1), 157-160.

- Bloch, F. (1953) 'The principle of nuclear induction', *Science*, 118(3068), 425-430.
- Bloch, F., Hansen, W. W. & Packard, M. (1946) 'The nuclear induction experiment', *Physical Review*, 70(7-8), 474-485.
- Bloembergen, N. & Pound, R. V. (1954) 'Radiation damping in magnetic resonance experiments', *Physical Review*, 95(1), 8-12.
- Blundell, C. D., DeAngelis, P. L. & Almond, A. (2006a) 'Hyaluronan: the absence of amide-carboxylate hydrogen bonds and the chain conformation in aqueous solution are incompatible with stable secondary and tertiary structure models', *Biochemical Journal*, 396(3), 487-498.
- Blundell, C. D., Reed, M. A. C. & Almond, A. (2006b) 'Complete assignment of hyaluronan oligosaccharides up to hexasaccharides', *Carbohydrate Research*, 341(17), 2803-2815.
- Bociek, S. M., Darke, A. H., Welti, D. & Rees, D. A. (1980) 'The <sup>13</sup>C-NMR spectra of hyaluronate and chondroitin sulphates. Further evidence on an alkali-induced conformation change', *European Journal of Biochemistry*, 109(2), 447-456.
- Borzacchiello, A. & Ambrosio, L. (2009). Structure-property relationships in hydrogels. In: Barbucci, R. (ed.) *Hydrogels - biological properties and applications*. Milan, Italy: Springer, 9-20.
- Bulpitt, P. & Aeschlimann, D. (1999) 'New strategy for chemical modification of hyaluronic acid: Preparation of functionalized derivatives and their use in the formation of novel biocompatible hydrogels', *Journal of Biomedical Materials Research*, 47(2), 152-169.
- Cowman, M. K., Lee, H. G., Schwertfeger, K. L., McCarthy, J. B. & Turley, E. A. (2015) 'The content and size of hyaluronan in biological fluids and tissues', *Frontiers in Immunology*, 6:261. doi: 10.3389/fimmu.2015.00261
- Cowman, M. K. & Matsuoka, S. (2005) 'Experimental approaches to hyaluronan structure', *Carbohydrate Research*, 340(5), 791-809.
- Crescenzi, V., Francescangeli, A., Renier, D. & Bellini, D. (2002) 'New cross-linked and sulfated derivatives of partially deacetylated hyaluronan: synthesis and preliminary characterization', *Biopolymers*, 64(2), 86-94.
- Csoka, A. B., Frost, G. I. & Stern, R. (2001) 'The six hyaluronidase-like genes in the human and mouse genomes', *Matrix Biology*, 20(8), 499-508.
- De Bouille, K., Glogau, R., Kono, T., Nathan, M., Tezel, A., Roca-Martinez, J. X., Paliwal, S. & Stroumpoulis, D. (2013) 'A review of the metabolism of 1,4-butanediol diglycidyl ether-crosslinked hyaluronic acid dermal fillers', *Dermatologic Surgery*, 39(12), 1758-1766.
- de Nooy, A. E. J., Capitani, D., Masci, G. & Crescenzi, V. (2000) 'Ionic polysaccharide hydrogels via the passerini and Ugi multicomponent condensations: Synthesis, behavior and solid-state NMR characterization', *Biomacromolecules*, 1(2), 259-267.
- DeAngelis, P. L. (2008) 'Monodisperse hyaluronan polymers: synthesis and potential applications', *Current Pharmaceutical Biotechnology*, 9(4), 246-248.
- DeAngelis, P. L., Jing, W., Drake, R. R. & Achyuthan, A. M. (1998) 'Identification and molecular cloning of a unique hyaluronan synthase from *Pasteurella multocida*', *Journal of Biological Chemistry*, 273(14), 8454-8458.
- Dicker, K. T., Gurski, L. A., Pradhan-Bhatt, S., Witt, R. L., Farach-Carson, M. C. & Jia, X. (2014) 'Hyaluronan: a simple polysaccharide with diverse biological functions', *Acta Biomaterialia*, 10(4), 1558-1570.

- Dische, Z. & Rothschild, C. (1967) 'Two modifications of the carbazole reaction of hexuronic acids for the differentiation of polyuronides', *Analytical Biochemistry*, 21(1), 125-130.
- Domon, B. & Costello, C. E. (1988) 'A systematic nomenclature for carbohydrate fragmentations in FAB-MS/MS spectra of glycoconjugates', *Glycoconjugate Journal*, 5(4), 397-409.
- Duan, J. & Kasper, D. L. (2011) 'Oxidative depolymerization of polysaccharides by reactive oxygen/nitrogen species', *Glycobiology*, 21(4), 401-409.
- Duus, J. Ø., Gotfredsen, C. H. & Bock, K. (2000) 'Carbohydrate structural determination by NMR spectroscopy: Modern methods and limitations', *Chemical Reviews*, 100(12), 4589-4614.
- Edsman, K., Nord, L. I., Öhrlund, Å., Lärkner, H. & Kenne, A. H. (2012) 'Gel properties of hyaluronic acid dermal fillers', *Dermatologic Surgery*, 38(7 Pt 2), 1170-1179.
- Emsley, J. W. & Feeney, J. (1995) 'Milestones in the first fifty years of NMR', *Progress in Nuclear Magnetic Resonance Spectroscopy*, 28(1), 1-9.
- Emsley, J. W. & Feeney, J. (2007) 'Forty years of progress in nuclear magnetic resonance spectroscopy', *Progress in Nuclear Magnetic Resonance Spectroscopy*, 50(4), 179-198.
- Fallacara, A., Baldini, E., Manfredini, S. & Vertuani, S. (2018) 'Hyaluronic acid in the third millennium', *Polymers*, 10(7):701. doi: 10.3390/polym10070701
- Feder-Davis, J., Hittner, D. M. & Cowman, M. K. (1991). Comparison of solution and solid-state structures of sodium hyaluronan by <sup>13</sup>C NMR Spectroscopy. In: Shalaby, W. S., McCormick, C. L. & Butler, G. B. (eds.) *Water-Soluble Polymers*. Washington, D.C., United States: American Chemical Society, 493-501.
- Fenn, J. B., Mann, M., Meng, C. K., Wong, S. F. & Whitehouse, C. M. (1989) 'Electrospray ionization for mass spectrometry of large biomolecules', *Science*, 246(4926), 64-71.
- Fraser, J. R. E. & Laurent, T. C. (1989) 'Turnover and metabolism of hyaluronan', *Ciba Foundation Symposia*, 143, 41-59.
- Gaidamauskas, E., Norkus, E., Butkus, E., Crans, D. C. & Grincienė, G. (2009) 'Deprotonation of β-cyclodextrin in alkaline solutions', *Carbohydrate Research*, 344(2), 250-254.
- Gaidamauskas, E., Norkus, E., Vaičiūnienė, J., Crans, D. C., Vuorinen, T., Jačiaskienė, J. & Baltrūnas, G. (2005) 'Evidence of two-step deprotonation of D-mannitol in aqueous solution', *Carbohydrate Research*, 340(8), 1553-1556.
- Gargiulo, V., Morando, M. A., Silipo, A., Nurisso, A., Pérez, S., Imberty, A., Cañada, F. J., Parrilli, M., Jiménez-Barbero, J. & De Castro, C. (2010) 'Insights on the conformational properties of hyaluronic acid by using NMR residual dipolar couplings and MD simulations', *Glycobiology*, 20(10), 1208-1216.
- Gibbs, D. A., Merrill, E. W., Smith, K. A. & Balazs, E. A. (1968) 'Rheology of hyaluronic acid', *Biopolymers*, 6(6), 777-791.
- Glish, G. L. & Burinsky, D. J. (2008) 'Hybrid mass spectrometers for tandem mass spectrometry', *Journal of the American Society for Mass Spectrometry*, 19(2), 161-172.
- Guarise, C., Pavan, M., Pirrone, L. & Renier, D. (2012) 'SEC determination of cross-link efficiency in hyaluronan fillers', *Carbohydrate Polymers*, 88(2), 428-434.
- Guss, J. M., Hukins, D. W. L., Smith, P. J. C., Winter, W. T., Arnott, S., Moorhouse, R. & Rees, D. A. (1975) 'Hyaluronic acid: Molecular conformations and interactions in two sodium salts', *Journal of Molecular Biology*, 95(3), 359-384.

- Han, L. & Costello, C. E. (2011) 'Electron transfer dissociation of milk oligosaccharides', *Journal of the American Society for Mass Spectrometry*, 22(6), 997-1013.
- Hargittai, I. & Hargittai, M. (2008) 'Molecular structure of hyaluronan: an introduction', *Structural Chemistry*, 19(5), 697-717.
- Haxaire, K., Braccini, I., Milas, M., Rinaudo, M. & Pérez, S. (2000) 'Conformational behavior of hyaluronan in relation to its physical properties as probed by molecular modeling', *Glycobiology*, 10(6), 587-594.
- Heatley, F. & Scott, J. E. (1988) 'A water molecule participates in the secondary structure of hyaluronan', *Biochemical Journal*, 254(2), 489-493.
- Hills, B. P., Takacs, S. F. & Belton, P. S. (1989) 'The effects of proteins on the proton NMR transverse relaxation times of water', *Molecular Physics*, 67(4), 903-918.
- Hoffman, A. S. (2012) 'Hydrogels for biomedical applications', *Advanced Drug Delivery Reviews*, 64, 18-23.
- Hofinger, E. S. A., Bernhardt, G. & Buschauer, A. (2007) 'Kinetics of Hyal-1 and PH-20 hyaluronidases: Comparison of minimal substrates and analysis of the transglycosylation reaction', *Glycobiology*, 17(9), 963-971.
- Holmbeck, S. M. A., Petillo, P. A. & Lerner, L. E. (1994) 'The solution conformation of hyaluronan: A combined NMR and molecular dynamics study', *Biochemistry*, 33(47), 14246-14255.
- Hovingh, P. & Linker, A. (1999) 'Hyaluronidase activity in leeches (*Hirudinea*)', *Comparative Biochemistry and Physiology Part B*, 124(3), 319-326.
- Huang, G. & Huang, H. (2018) 'Application of hyaluronic acid as carriers in drug delivery', *Drug Delivery*, 25(1), 766-772.
- Huin-Amargier, C., Marchal, P., Payan, E., Netter, P. & Dellacherie, E. (2006) 'New physically and chemically crosslinked hyaluronate (HA)-based hydrogels for cartilage repair', *Journal of Biomedical Materials Research Part A*, 76(2), 416-424.
- Huzarska, M., Ugalde, I., Kaplan, D. A., Hartmer, R., Easterling, M. L. & Polfer, N. C. (2010) 'Negative electron transfer dissociation of deprotonated phosphopeptide anions: Choice of radical cation reagent and competition between electron and proton transfer', *Analytical Chemistry*, 82(7), 2873-2878.
- Hyberts, S. G., Arthanari, H., Robson, S. A. & Wagner, G. (2014) 'Perspectives in magnetic resonance: NMR in the post-FFT era', *Journal of Magnetic Resonance*, 241, 60-73.
- Hyberts, S. G., Robson, S. A. & Wagner, G. (2013) 'Exploring signal-to-noise ratio and sensitivity in non-uniformly sampled multi-dimensional NMR spectra', *Journal of Biomolecular NMR*, 55(2), 167-178.
- Im, J. H., Song, J. M., Kang, J. H. & Kang, D. J. (2009) 'Optimization of medium components for high-molecular-weight hyaluronic acid production by *Streptococcus* sp. ID9102 via a statistical approach', *Journal of Industrial Microbiology & Biotechnology*, 36(11), 1337-1344.
- Ivarsson, I., Sandström, C., Sandström, A. & Kenne, L. (2000) '<sup>1</sup>H NMR chemical shifts of hydroxy protons in conformational analysis of disaccharides in aqueous solution', *Journal of the Chemical Society-Perkin Transactions 2*, (10), 2147-2152.
- Jedrzejak, M. J. (2000) 'Structural and functional comparison of polysaccharide-degrading enzymes', *Critical Reviews in Biochemistry and Molecular Biology*, 35(3), 221-251.

- Jedrzejas, M. J. & Stern, R. (2005) 'Structures of vertebrate hyaluronidases and their unique enzymatic mechanism of hydrolysis', *Proteins: Structure Function and Bioinformatics*, 61(2), 227-238.
- Jia, X., Colombo, G., Padera, R., Langer, R. & Kohane, D. S. (2004) 'Prolongation of sciatic nerve blockade by *in situ* cross-linked hyaluronic acid', *Biomaterials*, 25(19), 4797-4804.
- Johnson, C. S. (1999) 'Diffusion ordered nuclear magnetic resonance spectroscopy: principles and applications', *Progress in Nuclear Magnetic Resonance Spectroscopy*, 34(3), 203-256.
- Kablik, J., Monheit, G. D., Yu, L., Chang, G. & Gershkovich, J. (2009) 'Comparative physical properties of hyaluronic acid dermal fillers', *Dermatologic Surgery*, 35, 302-312.
- Kaneiwa, T., Mizumoto, S., Sugahara, K. & Yamada, S. (2010) 'Identification of human hyaluronidase-4 as a novel chondroitin sulfate hydrolase that preferentially cleaves the galactosaminidic linkage in the trisulfated tetrasaccharide sequence', *Glycobiology*, 20(3), 300-309.
- Karas, M., Bachmann, D., Bahr, U. & Hillenkamp, F. (1987) 'Matrix-assisted ultraviolet laser desorption of non-volatile compounds', *International Journal of Mass Spectrometry and Ion Processes*, 78, 53-68.
- Kazimierczuk, K. & Orekhov, V. (2015) 'Non-uniform sampling: post-Fourier era of NMR data collection and processing', *Magnetic Resonance in Chemistry*, 53(11), 921-926.
- Kemparaju, K. & Girish, K. S. (2006) 'Snake venom hyaluronidase: a therapeutic target', *Cell Biochemistry and Function*, 24(1), 7-12.
- Kenne, L., Gohil, S., Nilsson, E. M., Karlsson, A., Ericsson, D., Helander Kenne, A. & Nord, L. I. (2013) 'Modification and cross-linking parameters in hyaluronic acid hydrogels--definitions and analytical methods', *Carbohydrate Polymers*, 91(1), 410-418.
- Khunmanee, S., Jeong, Y. & Park, H. (2017) 'Crosslinking method of hyaluronic-based hydrogel for biomedical applications', *Journal of Tissue Engineering*, 8, doi: 10.1177/2041731417726464
- Kim, H., Jeong, H., Han, S., Beack, S., Hwang, B. W., Shin, M., Oh, S. S. & Hahn, S. K. (2017) 'Hyaluronate and its derivatives for customized biomedical applications', *Biomaterials*, 123, 155-171.
- Kiss, J. (1974).  $\beta$ -eliminative degradation of carbohydrates containing uronic acid residues. In: Tipson, R. S. & Horton, D. (eds.) *Advances in Carbohydrate Chemistry and Biochemistry*. Academic Press, 229-303.
- Knutson, C. A. & Jeanes, A. (1968) 'A new modification of the carbazole analysis: application to heteropolysaccharides', *Anal Biochem*, 24(3), 470-81.
- Krishnan, V. V. & Murali, N. (2013) 'Radiation damping in modern NMR experiments: Progress and challenges', *Progress in Nuclear Magnetic Resonance Spectroscopy*, 68, 41-57.
- Kudo, K. & Tu, A. T. (2001) 'Characterization of hyaluronidase isolated from *Agkistrodon contortrix contortrix* (southern copperhead) venom', *Archives of Biochemistry and Biophysics*, 386(2), 154-162.
- Köwitsch, A., Zhou, G. & Groth, T. (2018) 'Medical application of glycosaminoglycans: a review', *Journal of Tissue Engineering and Regenerative Medicine*, 12(1), e23-e41.

- Larrañeta, E., Henry, M., Irwin, N. J., Trotter, J., Perminova, A. A. & Donnelly, R. F. (2018) 'Synthesis and characterization of hyaluronic acid hydrogels crosslinked using a solvent-free process for potential biomedical applications', *Carbohydrate Polymers*, 181, 1194-1205.
- Laurent, T. C. (1987) 'Biochemistry of hyaluronan', *Acta Oto-Laryngologica*, 442, 7-24.
- Laurent, T. C. & Fraser, J. R. E. (1992) 'Hyaluronan', *The FASEB Journal*, 6(7), 2397-2404.
- Li, M., Rosenfeld, L., Vilar, R. E. & Cowman, M. K. (1997) 'Degradation of hyaluronan by peroxyxynitrite', *Archives of Biochemistry and Biophysics*, 341(2), 245-250.
- Liepinsh, E., Otting, G. & Wüthrich, K. (1992) 'NMR spectroscopy of hydroxyl protons in aqueous solutions of peptides and proteins', *Journal of Biomolecular NMR*, 2(5), 447-465.
- Linhardt, R. J., Galliher, P. M. & Cooney, C. L. (1986) 'Polysaccharide lyases', *Applied Biochemistry and Biotechnology*, 12(2), 135-176.
- Lowry, K. M. & Beavers, E. M. (1994) 'Thermal stability of sodium hyaluronate in aqueous solution', *Journal of Biomedical Materials Research*, 28(10), 1239-1244.
- Luo, Y., Kirker, K. R. & Prestwich, G. D. (2000a) 'Cross-linked hyaluronic acid hydrogel films: new biomaterials for drug delivery', *Journal of Controlled Release*, 69(1), 169-184.
- Luo, Y., Ziebell, M. R. & Prestwich, G. D. (2000b) 'A hyaluronic acid-taxol antitumor bioconjugate targeted to cancer cells', *Biomacromolecules*, 1(2), 208-218.
- Magalhães, M. R., da Silva, N. J. & Ulhoa, C. J. (2008) 'A hyaluronidase from *Potamotrygon motoro* (freshwater stingrays) venom: Isolation and characterization', *Toxicon*, 51(6), 1060-1067.
- Maleki, A., Kjøniksen, A. L. & Nyström, B. (2008) 'Effect of pH on the behavior of hyaluronic acid in dilute and semidilute aqueous solutions', *Macromolecular Symposia*, 274, 131-140.
- Mamyrin, B. A., Karataev, V. I., Shmikk, D. V. & Zagulin, V. A. (1973) 'The mass-reflectron, a new nonmagnetic time-of-flight mass spectrometer with high resolution', *Zhurnal Eksperimental'noi I Teoreticheskoi Fiziki*, 64(1), 82-89.
- Mandawe, J., Infanzon, B., Eisele, A., Zaun, H., Kuballa, J., Davari, M. D., Jakob, F., Elling, L. & Schwaneberg, U. (2018) 'Directed evolution of hyaluronic acid synthase from *Pasteurella multocida* towards high-molecular-weight hyaluronic acid', *Chembiochem*, 19(13), 1414-1423.
- Mareci, T. H. & Scott, K. N. (1977) 'Quantitative analysis of mixtures by carbon-13 nuclear magnetic resonance spectrometry', *Analytical Chemistry*, 49(14), 2130-2136.
- Meyer, K. & Palmer, J. W. (1934) 'The polysaccharide of the vitreous humor', *Journal of Biological Chemistry*, 107, 629-634.
- Mitra, A. K., Raghunathan, S., Sheehan, J. K. & Arnott, S. (1983) 'Hyaluronic acid: Molecular-conformations and interactions in the orthorhombic and tetragonal forms containing sinuous chains', *Journal of Molecular Biology*, 169(4), 829-859.
- Mobli, M. & Hoch, J. C. (2014) 'Nonuniform sampling and non-Fourier signal processing methods in multidimensional NMR', *Progress in Nuclear Magnetic Resonance Spectroscopy*, 83, 21-41.
- Mondek, J., Kalina, M., Simulescu, V. & Pekař, M. (2015) 'Thermal degradation of high molar mass hyaluronan in solution and in powder; comparison with BSA', *Polymer Degradation and Stability*, 120, 107-113.

- Moseley, R., Waddington, R. J. & Embery, G. (1997) 'Degradation of glycosaminoglycans by reactive oxygen species derived from stimulated polymorphonuclear leukocytes', *Biochimica et Biophysica Acta*, 1362(2-3), 221-231.
- Munson, M. S. B. & Field, F. H. (1966) 'Chemical ionization mass spectrometry .I. General introduction', *Journal of the American Chemical Society*, 88(12), 2621-2630.
- Nestor, G., Kenne, L. & Sandström, C. (2010) 'Experimental evidence of chemical exchange over the  $\beta(1\rightarrow3)$  glycosidic linkage and hydrogen bonding involving hydroxy protons in hyaluronan oligosaccharides by NMR spectroscopy', *Organic & Biomolecular Chemistry*, 8(12), 2795-2802.
- Nestor, G. & Sandström, C. (2017) 'NMR study of hydroxy and amide protons in hyaluronan polymers', *Carbohydrate Polymers*, 157, 920-928.
- Nguyen, S. & Fenn, J. B. (2007) 'Gas-phase ions of solute species from charged droplets of solutions', *Proceedings of the National Academy of Sciences of the United States of America*, 104(4), 1111-1117.
- Oommen, O. P., Wang, S., Kisiel, M., Sloff, M., Hilborn, J. & Varghese, O. P. (2013) 'Smart design of stable extracellular matrix mimetic hydrogel: Synthesis, characterization, and *in vitro* and *in vivo* evaluation for tissue engineering', *Advanced Functional Materials*, 23(10), 1273-1280.
- Park, K. Y., Kim, H. K. & Kim, B. J. (2013) 'Comparative study of hyaluronic acid fillers by *in vitro* and *in vivo* testing', *Journal of the European Academy of Dermatology and Venereology*, 28(5), 565-568.
- Paul, W. & Steinwedel, H. (1953) 'Ein neues massenspektrometer ohne magnetfeld', *Zeitschrift Für Naturforschung A*, 8(7), 448-450.
- Paul, W. & Steinwedel, H. (1960) *Apparatus for separating charged particles of different specific charges*. United States 2939952
- Pomin, V. H. (2014) 'Solution NMR conformation of glycosaminoglycans', *Progress in Biophysics and Molecular Biology*, 114(2), 61-68.
- Popov, K. I., Sultanova, N., Rönkkömäki, H., Hannu-Kuure, M., Jalonen, J., Lajunen, L. H. J., Bugaenko, I. F. & Tuzhilkin, V. I. (2006) ' $^{13}\text{C}$  NMR and electrospray ionization mass spectrometric study of sucrose aqueous solutions at high pH: NMR measurement of sucrose dissociation constant', *Food Chemistry*, 96(2), 248-253.
- Poppe, L., Stuikeprill, R., Meyer, B. & van Halbeek, H. (1992) 'The solution conformation of sialyl- $\alpha(2\rightarrow6)$ -lactose studied by modern NMR techniques and Monte Carlo simulations', *Journal of Biomolecular NMR*, 2(2), 109-136.
- Purcell, E. M. (1953) 'Research in nuclear magnetism', *Science*, 118(3068), 431-436.
- Purcell, E. M., Torrey, H. C. & Pound, R. V. (1946) 'Resonance absorption by nuclear magnetic moments in a solid', *Physical Review*, 69(1-2), 37-38.
- Rangaswamy, V. & Jain, D. (2008) 'An efficient process for production and purification of hyaluronic acid from *Streptococcus equi* subsp. *zooepidemicus*', *Biotechnology Letters*, 30(3), 493-496.
- Reháková, M., Bakoš, D., Soldán, M. & Vizárová, K. (1994) 'Depolymerization reactions of hyaluronic acid in solution', *International Journal of Biological Macromolecules*, 16(3), 121-124.

- Sandström, C., Baumann, H. & Kenne, L. (1998) 'The use of chemical shifts of hydroxy protons of oligosaccharides as conformational probes for NMR studies in aqueous solution. Evidence for persistent hydrogen bond interaction in branched trisaccharides', *Journal of the Chemical Society-Perkin Transactions 2*, (11), 2385-2393.
- Sattelle, B. M., Shakeri, J., Roberts, I. S. & Almond, A. (2010) 'A 3D-structural model of unsulfated chondroitin from high-field NMR: 4-sulfation has little effect on backbone conformation', *Carbohydrate Research*, 345(2), 291-302.
- Schaller-Duke, R. M., Bogala, M. R. & Cassady, C. J. (2018) 'Electron transfer dissociation and collision-induced dissociation of underivatized metallated oligosaccharides', *Journal of the American Society for Mass Spectrometry*, 29(5), 1021-1035.
- Schanté, C. E., Zuber, G., Herlin, C. & Vandamme, T. F. (2011) 'Chemical modifications of hyaluronic acid for the synthesis of derivatives for a broad range of biomedical applications', *Carbohydrate Polymers*, 85(3), 469-489.
- Scott, J. E. (1989) 'Secondary structures in hyaluronan solutions: Chemical and biological implications', *Ciba Foundation Symposia*, 143, 6-20.
- Scott, J. E., Heatley, F. & Hull, W. E. (1984) 'Secondary structure of hyaluronate in solution', *Biochemical Journal*, 220(1), 197-205.
- Segura, T., Anderson, B. C., Chung, P. H., Webber, R. E., Shull, K. R. & Shea, L. D. (2005) 'Crosslinked hyaluronic acid hydrogels: a strategy to functionalize and pattern', *Biomaterials*, 26(4), 359-371.
- Shaka, A. J., Keeler, J., Frenkiel, T. & Freeman, R. (1983) 'An improved sequence for broad-band decoupling: WALTZ-16', *Journal of Magnetic Resonance*, 52(2), 335-338.
- Shapiro, Y. E. (2011) 'Structure and dynamics of hydrogels and organogels: An NMR spectroscopy approach', *Progress in Polymer Science*, 36(9), 1184-1253.
- Sheehan, J. K. & Atkins, E. D. T. (1983) 'X-ray fiber diffraction study of conformational changes in hyaluronate induced in the presence of sodium, potassium and calcium cations', *International Journal of Biological Macromolecules*, 5(4), 215-221.
- Shu, X. Z., Liu, Y., Luo, Y., Roberts, M. C. & Prestwich, G. D. (2002) 'Disulfide cross-linked hyaluronan hydrogels', *Biomacromolecules*, 3(6), 1304-1311.
- Stern, R. (2004) 'Hyaluronan catabolism: a new metabolic pathway', *European Journal of Cell Biology*, 83(7), 317-325.
- Stern, R., Asari, A. A. & Sugahara, K. N. (2006) 'Hyaluronan fragments: an information-rich system', *European Journal of Cell Biology*, 85(8), 699-715.
- Stern, R., Kogan, G., Jedrzejewski, M. J. & Šoltés, L. (2007) 'The many ways to cleave hyaluronan', *Biotechnology Advances*, 25(6), 537-557.
- Stern, R. & Maibach, H. I. (2008) 'Hyaluronan in skin: aspects of aging and its pharmacologic modulation', *Clinics in Dermatology*, 26(2), 106-122.
- Sze, J. H., Brownlie, J. C. & Love, C. A. (2016) 'Biotechnological production of hyaluronic acid: a mini review', *3 Biotech*, 6(1):67. doi: 10.1007/s13205-016-0379-9
- Takano, R. (2002) 'Desulfation of sulfated carbohydrates', *Trends in Glycoscience and Glycotechnology*, 14(80), 343-351.

- Taylor, R. E. & Peterson, R. D. (2010) 'Comparison of spin-lattice relaxation measurements made in the presence of strong radiation damping', *Journal of Molecular Structure*, 970(1), 155-159.
- Tezel, A. & Fredrickson, G. H. (2008) 'The science of hyaluronic acid dermal fillers', *Journal of Cosmetic and Laser Therapy*, 10(1), 35-42.
- Tian, G. X., Sun, X., Bai, J. K., Dong, J. H., Zhang, B., Gao, Z. Q. & Wu, J. L. (2019) 'Doxorubicin-loaded dual-functional hyaluronic acid nanoparticles: Preparation, characterization and antitumor efficacy *in vitro* and *in vivo*', *Molecular Medicine Reports*, 19(1), 133-142.
- Tiwari, S. & Bahadur, P. (2019) 'Modified hyaluronic acid based materials for biomedical applications', *International Journal of Biological Macromolecules*, 121, 556-571.
- Tomihata, K. & Ikada, Y. (1997a) 'Crosslinking of hyaluronic acid with glutaraldehyde', *Journal of Polymer Science: Part A: Polymer Chemistry*, 35(16), 3553-3559.
- Tomihata, K. & Ikada, Y. (1997b) 'Preparation of cross-linked hyaluronic acid films of low water content', *Biomaterials*, 18(3), 189-195.
- Tømmeraaas, K. & Wahlund, P. O. (2009) 'Poly-acid properties of biosynthetic hyaluronan studied by titration', *Carbohydrate Polymers*, 77(2), 194-200.
- Wang, H. M., Loganathan, D. & Linhardt, R. J. (1991) 'Determination of the pK<sub>a</sub> of glucuronic acid and the carboxy groups of heparin by <sup>13</sup>C-nuclear-magnetic-resonance spectroscopy', *Biochemical Journal*, 278, 689-695.
- Vliegenthart, J. F. G., Dorland, L. & van Halbeek, H. (1983) 'High-resolution, <sup>1</sup>H-nuclear magnetic resonance spectroscopy as a tool in the structural analysis of carbohydrates related to glycoproteins', *Advances in Carbohydrate Chemistry and Biochemistry*, 41, 209-374.
- Wolff, J. J., Leach, F. E., Laremore, T. N., Kaplan, D. A., Easterling, M. L., Linhardt, R. J. & Amster, I. J. (2010) 'Negative electron transfer dissociation of glycosaminoglycans', *Analytical Chemistry*, 82(9), 3460-3466.
- Wu, D. H., Chen, A. D. & Johnson, C. S. (1995) 'An improved diffusion-ordered spectroscopy experiment incorporating bipolar-gradient pulses', *Journal of Magnetic Resonance, Series A*, 115(2), 260-264.
- Yuan, P., Lv, M., Jin, P., Wang, M., Du, G., Chen, J. & Kang, Z. (2015) 'Enzymatic production of specifically distributed hyaluronan oligosaccharides', *Carbohydrate Polymers*, 129, 194-200.
- Yuki, H. & Fishman, W. H. (1962) 'Purification and characterization of leech hyaluronic acid-endo-β-glucuronidase', *Journal of Biological Chemistry*, 238(5), 1877-1879.
- Zakeri, A., Rasaee, M. J. & Pourzardosht, N. (2017) 'Enhanced hyaluronic acid production in *Streptococcus zooepidemicus* by over expressing HasA and molecular weight control with Niscin and glucose', *Biotechnology Reports*, 16, 65-70.
- Zambrello, M. A., Schuyler, A. D., Maciejewski, M. W., Delaglio, F., Bersonova, I. & Hoch, J. C. (2018) 'Nonuniform sampling in multidimensional NMR for improving spectral sensitivity', *Methods*, 138, 62-68.
- Ågerup, B. (1998) *Polysaccharide gel composition*. United States 5827937
- Öhrlund, J. Å. & Edsman, K. L. M. (2015) 'The myth of the "biphasic" hyaluronic acid filler', *Dermatologic Surgery*, 41(12), S358-S364.

## Popular science summary

Hyaluronic acid "HA" is a naturally occurring polysaccharide, which is a long chain of sugar molecules (monosaccharides) consisting of short repeating units. The repeating unit of hyaluronic acid is a disaccharide consisting of a glucuronic acid and an acetylated glucosamine. Hyaluronic acid is found in all tissues and tissue fluids of vertebrates. A person weighing 70 kg has about 15 g of hyaluronic acid in the body of which about half is found in the skin. HA has many important biological functions. Due to the special properties of hyaluronic acid (*e.g.* high water absorption capacity, high viscoelasticity, biocompatibility), it is widely used for various biomaterials.

Hydrogels consist of networks of cross-linked polymers which can hold large volumes of water. The cross-links may be either chemical or physiological (*e.g.* entanglements).

The studies in this work have mainly been carried out using two analytical techniques i) nuclear magnetic resonance "NMR" spectroscopy, and ii) mass spectrometry "MS". Both techniques are used to study molecular structures. NMR spectroscopy analyses how atomic nuclei behave in a strong static magnetic field when disturbed from equilibrium by another temporary magnetic field. Depending on the chemical environment of the atomic nuclei, they emit different signals that provide information on the interaction between the atoms. By interpreting the results, it is revealed how the atoms are linked together and how they relate to each other in space. Mass spectrometry provides information on the mass of molecules, it is also possible to break the molecules into smaller pieces (fragments) and analyse the mass of the pieces. By studying the various masses, information about the structure of the molecule is obtained.

In this thesis, I have studied hydrogels of chemically cross-linked hyaluronic acid. The cross-linker molecule that has been used is shortened BDDE and is a diepoxide. The properties of the gels will be correlated to their structure and it is therefore important to have analytical methods to study the structure.

For each repeating unit of hyaluronic acid, there are four different hydroxy groups that can react with BDDE. From NMR and MS analysis, we identified that BDDE bind to all four positions. One of the positions (carbon number four of the aminoglycan) was more common than the others.

While performing the investigation to determine where the cross-linker is located, we found specific NMR signals for each of the four positions. We then used these signals to create a simple NMR method to determine the distribution of cross-linkers at the four different positions.

In the cross-linking reaction, the cross-linker can either bind to two hyaluronic acid chains and thus create a cross-link or to one chain only and create a pendant cross-linker. It is important to know the amount of cross-linkers that have reacted and how large proportion of real cross-links that has been formed since it affects the properties of the gel. We identified signals in the carbon NMR spectra that could be related to the total number of cross-linkers and to the number of pendent cross-linkers and were able to further develop a method for analysing these parameters.

To investigate the reason for the observed distribution of cross-linkers on hyaluronic acid, we investigated the reactivity of the various hydroxyl groups. This was performed by a comparative study with desulphated chondroitin. Chondroitin is a polysaccharide which has a repeating unit very similar to that of hyaluronic acid. We compared i) the distribution of cross-linker ii) the influence of pH on the polysaccharide NMR, and signals iii) hydrogen bonds. The difference in structure between hyaluronic acid and chondroitin was reflected in all parameters studied.

Finally, we studied the dynamic properties of water in various hyaluronic acid hydrogels and solutions. The behaviour of the water molecules reflected the concentration and molecular weight of hyaluronic acid. Some correlation to the strength of the hydrogels could also be determined.

## Populärvetenskaplig sammanfattning

Hyaluronsyra "HA" är en naturligt förekommande polysackarid, det är en lång kedja av socker molekyler (monosackarider) som består av korta repeterande enheter. Den repeterande enheten i hyaluronsyra är en disackarid som utgörs av en glukuronsyra och en acetylerad glukosamin. Hyaluronsyra finns i alla vävnader och vävnadsvätskor hos ryggradsdjur. En människa som väger 70 kg har ungefär 15 g hyaluronsyra i kroppen varav ungefär hälften återfinns i huden. Hyaluronsyra har många viktiga biologiska funktioner. På grund av hyaluronsyrans speciella egenskaper (hög vattenupptagningsförmåga, hög viskoelasticitet, biokompatibilitet) så används den flitigt till olika biomaterial.

Hydrogeler består av nätverk av tvärbundna polymerer som kan innehålla stora volymer vatten. Tvärbindingarna kan vara antingen kemiska eller fysiologiska (t.ex. hoptrasslingar).

Två analystekniker har i huvudsak använts för studierna i detta arbete i) kärnmagnetisk resonansspektroskopi, "NMR-spektroskopi" och ii) masspektrometri "MS". Båda teknikerna kan användas för att studera molekyllära strukturer. NMR-spektroskopi analyserar hur atomkärnor beter sig i ett starkt statiskt magnetfält när de störs från jämvikt av ett annat tillfälligt magnetfält. Beroende på atomkärnornas kemiska omgivning avger de olika signaler som ger information om atomernas samverkan med varandra. Genom att tolka resultaten går det att se hur atomerna sitter ihop och även hur de förhåller sig till varandra i rymden. Masspektrometri ger information om molekylers massa, det går även att bryta sönder molekylerna (fragmentera) i mindre bitar och analysera bitarnas massa. Genom att studera de olika massorna erhålls information om molekylens struktur.

I den här avhandlingen har jag studerat hydrogeler av kemiskt tvärbunden hyaluronsyra. Tvärbindarmolekylen som har använts förkortas BDDE och är en diepoxid. Hydrogelernas egenskaper beror på deras struktur och det är därför viktigt att ha analytiska metoder för att studera strukturerna.

För varje repeterande enhet av hyaluronsyra finns det fyra olika hydroxigrupper som BDDE kan binda till. Via NMR-spektroskopi och MS-analys identifierade vi att BDDE kan binda till samtliga fyra positioner. En av dessa positioner (hydroxigruppen på kol nummer fyra på aminoglykanen) var vanligare än de andra. När vi gjorde utredningen för att avgöra var tvärbindaren sitter hittade vi specifika NMR-signaler för var och en av de fyra positionerna. Dessa signaler använde vi sedan för att skapa en enkel NMR-metod för att bestämma fördelningen av tvärbindare på de fyra olika positionerna.

Vid tvärbindningsreaktionen kan tvärbindaren antingen binda till två hyaluronsyrakedjor och på så sätt skapa en tvärbinding eller bara till en kedja och skapa en fritt hängande tvärbindare. Det är viktigt att veta hur många tvärbindare som reagerat samt hur stor andel riktiga tvärbindningar som bildats eftersom det påverkar gelens egenskaper. Vi identifierade signaler i kol-NMR-spektrumet som kunde relateras till det totala antalet tvärbindare samt till antalet fritt hängande tvärbindare, och kunde därmed utveckla en metod för att analysera dessa parametrar.

För att undersöka varför fördelningen av tvärbindare på hyaluronsyra ser ut som den gör undersökte vi också reaktiviteten hos de olika hydroxygrupperna. Detta utfördes genom en jämförande studie med ickesulfaterad kondroitin. Kondroitin är en polysackarid som har en repeterande enhet som är väldigt lik hyaluronsyrans. Vi jämförde i) fördelningen av tvärbindare ii) inverkan av pH på polysackaridens NMR-signaler och iii) vätebindningar. Skillnaden i struktur mellan hyaluronsyra och kondroitin återspeglades i alla undersökta parametrar.

Slutligen studerade vi vattnets dynamiska egenskaper i olika hydrogeler och lösningar av hyaluronsyra. Vattnets beteende reflekterade hyaluronsyrans koncentration och molekylvikt. En viss korrelation till hydrogelernas styrka kunde också påvisas.

## Acknowledgements

I would like to express my most sincere gratitude to all of you wonderful people who supported me during my years as a PhD student.

First, to my main supervisor Corine Sandström you are a true inspiration and a great role model. Apart from being an excellent scientist, you have a heart of gold and I am so thankful for everything you have taught me and all the support you have given me. You always manage to think positive and in terms of solutions even when obstacles appear. Thank you for believing in me.

My perpetual officemate, Suresh Gohil, thank you for not retiring, I do not know what I would have done without you. My MS guru! Thank you for everything you have taught me and for your kindness and sense of humor.

My co-supervisor Jan Eriksson, thank you for trying so hard to produce negative results with me. Although we did not get the results we hoped for I learned a lot. I really appreciate your attention to detail, thank you for always being so calm and happy.

My co-supervisor Lars Nord. First, thank you for accepting me and supervising me during my master thesis, and second thank you for encouraging me to do a PhD. Thank you also for labelling everything so carefully when you were at the department 15 years ago, it was nice to know which ruler, chemicals *etc.* you had used.

The most current addition in my supervisor group, Gustav Nestor. You were also a PhD student here when I started, I remember you as very polite and helpful. After gaining some confidence in Pittsburgh you came back and became my co-supervisor. A big thank you to the great effort you put into proof reading this thesis, your comments definitely improved it.

I would also very much like to thank Galderma for funding my PhD project. Thank you to all of my co-authors; Anne Helander Kenne, Anders Karlsson, Hotan Mojarradi, Jean-Guy Boiteau and Thibaud Gerfaud. Special thank you also to Kerstin Baumann, Morgan Karlsson and Åke Öhrlund. Moreover, thank

you to all of the other wonderful people at Galderma both former co-workers and new acquaintances.

Lena Lundqvist, it is not an understatement to say that I could not have done this without you. You have always been there for me, to laugh with, cry with, when I needed to rant or when I just needed a hug. You picked me up and made me believe in myself. I am forever grateful. We were fat (pregnant) together and now our two amazing daughters are friends as well.

Christina Nord your crazy and sick humor will haunt me forever (mission accomplished I guess?). All jokes aside, I always appreciate your company, you are a very kind person and even though I might never have told you, I am happy that you were forced to become my officemate. Thank you for nice discussions, shared laughs and all the Christmas decorations.

Hanna Eriksson Röhnisch, we have taught many courses together, ate many “lunches” together and had many laughs together. I will never forget when you ordered 1 000 000 pipette tips, that still makes me laugh. That you thought I was 40 when you started... Not so much. Johnny Östman, since you joined our lunches you have contributed to a lot of... interesting? discussion topics. I owe you both a lot of cookies, thank you for help and support.

Welcome to the group to Elin Alexandersson and Yan Xue. Good luck on your coming adventure, it is a roller coaster I assure you, so buckle up and try enjoy the ride even if the valleys sometimes are deep and the turns can be sharp once you make it to the end it will be worth it. Thank you to Anja Herneke, Klara Nilsson and Solja Pietiäinen for present pleasant company in the lunchroom, good luck on your continued PhD studies. Fredric Svensson, I do not know why you avoid eating lunch with us, you always laugh so much when you do.

My former officemates David Hansson and Pierre Andersson, thank you for guidance when I was new here. Moreover, thank you to all of the other PhD students who was here when I started and welcomed me as a part of the group. Eric Morssing Vilén, Kai Wilkinsson, Shahin Norbaksh, Johan Mähler, Lars Eklund and Tobias Bölscher. Also thank you to those who started after me but finished before me Martin Palmqvist and Elizabeth Polida Legaria.

Thank you to Anders Sandström for giving me the opportunity to teach and for always having a smile on your face.

To Vadim Kessler, I know I maybe was nagging you a little bit hard about the “stickande och skärande” things in your lab but you eventually learned which means you listened. Thank you for being a good head of department.

Thanks to Henrik Hansson for being a good co-safety officer for many years. No sever accidents occurred so I render we did a good job.

To all of my other colleges (past and present) here at the department I would like to say thank you for making it a joy to come to work. Anke, Anders, Daniel,

Gunnar, Karin, Eva, Ievgen, Kerstin, Alyona, Pernilla, Maud, Rosana, Simon, Gulaim, Ingmar, Ali, Elisabeth, Xue, Jule, Mikolaj, Abhijeet, Hasitha, Jolanta, Bernt, Sonja, and also all of you that I accidentally forgot.

Stort tack till alla K05:or som förgyllde mina år som student och speciellt till er som fortsatt förgylla min tillvaro genom att vara mina vänner.

Från Skellefte vill jag tacka alla mina "gamla" vänner men speciellt tack till Malin Lövgren för att du är du och Hanna Persson för att du är så go och glad.

Tack till min mamma och pappa, världens bästa mamma Ingmarie och pappa Göran. Tack för att ni alltid stöttat mig och trott på mig. Tack för att ni kommer och hälsar på så ofta som ni kan även om det är långt att färdas, det betyder mycket för mig och det är alltid en energiboost att ha er här. Ni är för övrigt också världens bästa mormor och morfar.

Tack till mina systrar Clara, Sanna och Hilda. Vi är fyra väldigt olika systrar fast vi har alla våra gemensamma punkter. Jag är så glad och tacksam över att ha er och era familjer i mitt liv, ni är helt fantastiska.

Till sist vill jag tacka min man Michel för att du stöttade mig i beslutet att bli doktorand och för att du gett mig det absolut finaste jag har, våra tre underbara barn William, Douglas och Olivia. Denna avhandling är tillägnad er, jag älskar er mer än vad ord kan beskriva.

